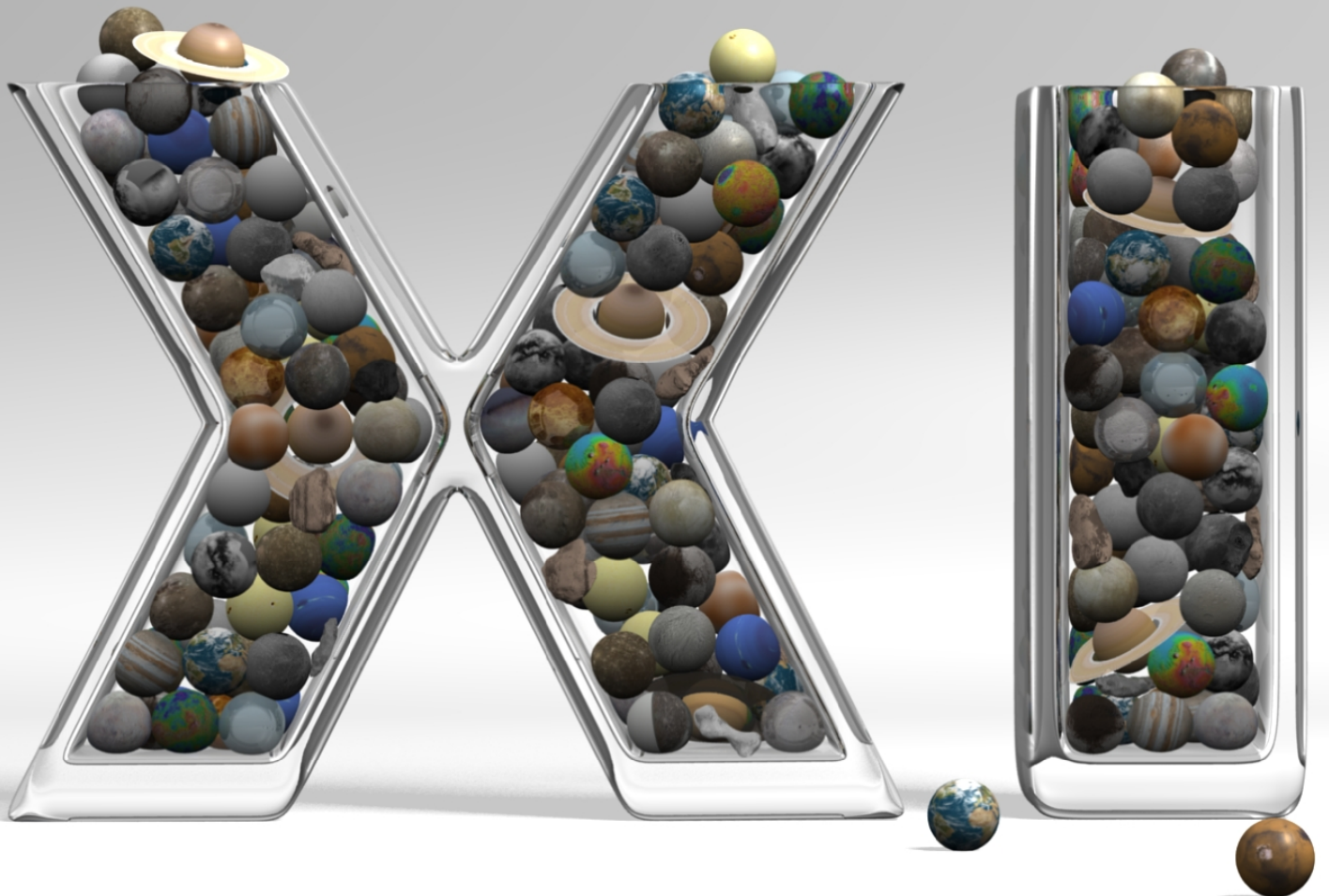


Proceedings of the
11th LPLC
The 2008 Lunar and Planetary
Laboratory Conference



Proceedings of the Lunar and Planetary Conference XI

May 19-20, 2008
Hacienda del Sol
Tucson, Arizona

<i>Conference Schedule</i>	<i>II</i>
<i>Conference Welcome</i>	<i>VI</i>
<i>Science Abstracts, May 19</i>	
<i>Planetary Surfaces</i>	<i>1</i>
<i>Observation</i>	<i>4</i>
<i>Mars</i>	<i>6</i>
<i>Meteorites</i>	<i>10</i>
<i>User Demonstrations</i>	<i>14</i>
<i>Origins and Formation</i>	<i>17</i>
<i>Technical Abstracts, May 19</i>	
<i>Systems and Languages</i>	<i>21</i>
<i>Web Applications and Mission Planning Software</i>	<i>23</i>
<i>Data Archive</i>	<i>26</i>
<i>Data Analysis and Concurrency</i>	<i>29</i>
<i>Science Abstracts, May 20</i>	
<i>Dynamics</i>	<i>32</i>
<i>Atmospheres</i>	<i>36</i>
<i>Space Physics</i>	<i>38</i>
<i>Terrestrial Planets and Titan</i>	<i>42</i>
<i>Craters and Impacts</i>	<i>46</i>
<i>Satellites</i>	<i>49</i>
<i>Keynote</i>	<i>52</i>

Monday, May 19th – Casa Feliz Room

8:30	Registration and Breakfast	E. Chollet, D. Minton, E. Palmer
9:00	Planetary Surfaces	Chair: D. Minton
	Modeling a Dune Field	S. Diniega* and K. Glasner
	Megafloods	V. Baker*
9:30	Observation	Chair: D. Minton
	Asteroid Occultations: Video Techniques	J. McGaha*
	Enumeration of the Degenerates in the Solar Neighborhood	J. Holberg*
10:00	Break	
10:15	Mars	Chair: D. Choi
	Phoenix Payload Instruments	P. Woida*
	HiRISE Observations of Fractured Mounds on Mars	C. Dundas* and A. McEwen
	Enrichment of Argon over Mars' Winter Poles: Indicators of Peculiar Atmosphere Dynamics	W. Boynton* and A. Sprague
	Wet Chemistry Lab on Phoenix	S. Young*
	Production of Soils and the Shielding Effect of Small-Scale Surface Features (Invited)	J. Moores*
11:45	Lunch	
1:00	Meteorites	Chair: K. Kolb
	A Comprehensive Observational Survey of CR Chondrite Type-II Chondrules and Matrix	D. Schrader*, D. Lauretta, H. Connolly Jr.
	Metal/Olivine Partitioning Experiments as an Aid to Defining the Cooling Rate of Pallasites	E. Hill*, K. Domanik, G. Huss, M. Drake
	MIL 05029: An L-Melt Rock from the Early Solar System	J. Weirich*
	Relationships among Ungrouped Primitive Achondrites and Type-7 Ordinary Chondrites	K. Gardner-Vandy* and D. Lauretta
2:00	Break	
2:15	User Demonstrations	Chair: C. Schaller
	Jbody User Demo	D. Lytle*
	HiReport	G. McArthur*
	Obtaining and Understanding HiRISE Images	E. Eliason* and HiRISE Operations Team
3:15	Break	
3:30	Origins and Formation	Chair: K. Gardner-Vandy
	Adsorption as a Source of Water in the Inner Solar System: A Kinetic Monte Carlo Study	K. Muralidharan*, M. Stimpfl, P. Deymier, M. Drake
	Photolytic Generation of Carbon Dioxide on Iapetus	E. Palmer* and R. Brown
	Problems with the Snowball Recovery Mechanism, Applications for Planetary Habitability	A. Pavlov*
	Low-Temperature Sulfides in Stardust: TEM Analysis of a Sphalerite/Pyrrhotite Assemblage from Track 7	E. Berger*, L. Keller, D. Joswiak, G. Matrajt, D. Lauretta



Monday, May 19th – Hacienda Room

8:30	Registration and Breakfast	E. Chollet, D. Minton, E. Palmer
9:00	Systems	Chair: C. Schaller
	DNS – A Glue of the Internet and Much More	T. Spriggs*
	Massive Storage on the Cheap	J. Plassmann*, D. Jones, T. Spriggs, T. Forrester
10:00	Languages	Chair: C. Schaller
	Secure Client-Server Authentication in Java	A. Davidson*
10:30	Break	
10:45	Web Applications	Chair: C. Schaller
	Reusability in Web Applications	G. McArthur*
	Load Testing the Web Application Stack: How do you Know your Web Application can Handle the Load?	R. Heyd*
11:15	Mission Planning Software	Chair: C. Schaller
	Extending JMARS for HiRISE Science Planning and Beyond	C. Schaller*
11:30	Lunch	
12:30	Data Archive	Chair: C. Schaller
	Managing Versions of Science Data Products Using Databases and Software Tools	R. Heyd*
	PDS_JP2	B. Castalia*, A. Davidson, B. Pearson
1:00	Data Analysis	Chair: C. Schaller
	Jbody: A Planetray Body Data Analysis Tool	D. Lytle*, V. Pasek, J. Ivens, R. Watson
1:15	Concurrency	Chair: C. Schaller
	Stage_Manager	B. Castalia* and A. Davidson

Tuesday, May 20th – Casa Feliz Room

8:30	Registration and Breakfast	E. Chollet, D. Minton, E. Palmer
9:00	Dynamics	Chair: E. Berger
	Possible Discrepancy in the Number Distribution of Asteroids in the Main Belt	D. Minton* and R. Malhotra
	OGLE-2006-BLG-109L: A Solar System Look-alike	R. Malhotra* and D. Minton
	In the Groove: Mean Motion Resonances between Centaurs and the Giant Planets	B. Bailey* and R. Malhotra
	The Problem of Producing High-Perihelion Kuiper Belt Objects	K. Volk*
10:00	Atmospheres	Chair: E. Berger
	Assessment of Saturn's Atmosphere and Zonal Winds from Cassini/VIMS	D. Choi*, A. Showman, R. Brown
	The Origin of Oxygen Species in Titan's Atmosphere	S. Hörst*, V. Vuitton, R. Yelle
10:30	Break	
10:45	Space Physics	Chair: K. Volk
	Examining Solar Energetic Particle Diffusion through Dropout Observations	E. Chollet* and J. Giacalone
	The Effect of Interplanetary Turbulence on Solar Energetic Particles	J. Giacalone*
	Solar Cycle Dependence of Umbral Brightness and Magneto-Induced Line Broadening	T. Schad*
	Propagation of Impulsive Solar Energetic Particles in Large-Scale Turbulence	F. Guo* and J. Giacalone
	Energetic Ions and Atoms from the Solar Wind Termination Shock	J. Kota*
12:00	Lunch	
1:15	Terrestrial Planets	Chair: C. Dundas
	Terrestrial Planet Formation: New Insights and Outstanding Questions (Invited)	D. O'Brien*
1:45	Titan	Chair: C. Dundas
	Titan's Rain, Raindrops, and Dewdrops: Descent Imager / Spectral Radiometer Observations	E. Karkoschka* and M. Tomasko
	Cassini Imaging of Titan and the Saturnian System	J. Perry*
	Hydrolysis of Laboratory Made Tholins in Ammonia-Water Solutions	C. Neish*, Á. Somogyi, J. Lunine, M. Smith
2:30	Craters and Impacts	Chair: C. Dundas
	Atmospheric Dispersion of Small Impactors on Mars	H.J. Melosh*, B. Ivanov, A. McEwen.
	Bolide Impact as a Mechanism for Formation of Chaos Terrain on Europa	R. Cox*, L. Ong, M. Arakawa
3:00	Break	
3:15	Satellites	Chair: C. Neish
	Topography of Chaotic Terrain on Europa	R. Greenberg*, T. Hurford, K. Varland, M. Foley
	Mission Concept: Io Volcano Observer (IVO)	A. McEwen* and the IVO Team
	Astrobotic and the Quest for the Google Lunar X-Prize	D. Lauretta*



Tuesday, May 20th – Casa Feliz Room

4:00 **Keynote – Icy Satellites: 400 Years of Discovery**

Guest Speaker: Michael Bland

5:00 **Reception**

Welcome to the 11th Lunar and Planetary Laboratory Conference

Eileen Chollet, David Minton, and Eric Palmer
2008 Lunar and Planetary Laboratory Conference Organizing Committee

Welcome to the eleventh annual Lunar and Planetary Laboratory Conference, at the Hacienda del Sol resort in Tucson Arizona, May 19th and 20th 2008. We have a great turnout this year, with just over fifty talks scheduled.

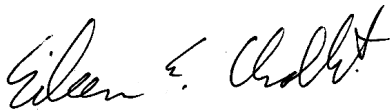
We are once again running a parallel technical session, to be held on Monday, May 19th. In addition, we have included a new science session, called User Demonstrations, for the purpose of demonstrating some of the unique software tools being developed here at LPL that we believe will be useful for scientific research.

The abstract booklet will only be available electronically this year. We have retained a printer-friendly layout, similar in format to those

of previous years.

Most talks will be scheduled for 15 minutes, allowing for a 10-minute talk and 5 minutes for questions. In addition, two recent LPL graduate have been invited to give 30-minute talks. The conference will be concluded with an hour-long keynote address by recent graduate, Michael Bland, titled "Icy Satellites: 400 years of discovery."

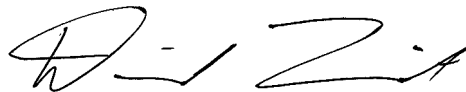
Finally, we would like to thank all of the speakers. This conference is a unique way for members of our department to share with each other the incredible breadth of activities that take place here at LPL. Without your contributions, this conference would not be possible.



Eileen Chollet



Eric Palmer



David Minton

Planetary Surfaces

May 19
9:00AM – 9:30AM

Chair: D. Minton

<i>Conference Schedule</i>	II
<i>Conference Welcome</i>	VI
<i>Science Abstracts, May 19</i>	
Planetary Surfaces	1
<i>Observation</i>	4
<i>Mars</i>	6
<i>Meteorites</i>	10
<i>User Demonstrations</i>	14
<i>Origins and Formation</i>	17
<i>Technical Abstracts, May 19</i>	
<i>Systems and Languages</i>	21
<i>Web Applications and Mission Planning Software</i>	23
<i>Data Archive</i>	26
<i>Data Analysis and Concurrency</i>	29
<i>Science Abstracts, May 20</i>	
<i>Dynamics</i>	32
<i>Atmospheres</i>	36
<i>Space Physics</i>	38
<i>Terrestrial Planets and Titan</i>	42
<i>Craters and Impacts</i>	46
<i>Satellites</i>	49
<i>Keynote</i>	52

Modeling a Dune Field

S. Diniega* and K. Glasner

Presenting and Corresponding Author: serina@lpl.arizona.edu

The aim of this work was to construct a transverse (2-dimensional) dune field model, beginning with a smaller scale 2-dimensional model of dune evolution and then compiling statistics about dune-dune interactions to move up to the larger scale dune field problem. Although just an elementary start, this study begins to address the open question about whether, in the presence of steady environmental conditions, dune fields exhibit self-organizing behavior or will continually coalesce. It has been shown that in

considering collision-derived dune field dynamics, different mass exchange functions will yield strikingly different behaviors. Additionally, the use of different boundary or initial conditions can have a large effect on the results of the model. This clearly demonstrates that more experiment- or observation-based data is needed to help calibrate and/or validate how a dune field model is arranged, and care needs to be taken when interpreting the results of such models.

Megafloods

V. Baker*

Presenting and Corresponding Author: baker@hwr.arizona.edu

The surface of Mars preserves landforms associated with the largest known water floods. While most of these megafloods occurred more than one billion years ago, recent spacecraft images document a phase of outburst flooding and associated volcanism that seems no older than tens of millions of years. The megafloods that formed the Martian outflow channels had maximum discharges comparable to those of Earth's ocean currents and its thermohaline circulation. On both Earth and Mars, abrupt and episodic operation of these mega-scale processes have been major factors in global climatic change. On relatively short time scales, by their influence on oceanic circulation, Earth's Pleistocene megafloods probably (1) induced the Younger Dryas cooling of 12.8 thousand years ago, and (2) initiated the Bond cycles of ocean-climate oscillation with their associated Heinrich events of "iceberg armadas" into the North Atlantic. The Martian megafloods are hypothesized to have induced the episodic formation of a northern plains "ocean", which,

with contemporaneous volcanism, led to relatively brief periods of enhanced hydrological cycling on the land surface (the "MEGAOUTFLO Hypothesis"). This process of episodic short-duration climate change on Mars, operating at intervals of hundreds of millions of years, has parallels in the Neoproterozoic glaciation of Earth (the "Snowball Earth Hypothesis"). Both phenomena are theorized to involve abrupt and spectacular planet-wide climate oscillations, and associated feedbacks with ocean circulation, land-surface weathering, glaciation, and atmospheric carbon dioxide. The critical factors for mega-scale environmental change on both Mars and Earth seem to be associated tectonics and volcanism, plus the abundance of water for planetary cycling. Some of the most important events in planetary history, including those of the biosphere, seem to be tied to cataclysmic episodes of massive hydrological change.

Observation

May 19
9:30AM – 10:00AM

Chair: D. Minton

<i>Conference Schedule</i>	<i>II</i>
<i>Conference Welcome</i>	<i>VI</i>
<i>Science Abstracts, May 19</i>	
<i>Planetary Surfaces</i>	<i>1</i>
Observation	4
<i>Mars</i>	<i>6</i>
<i>Meteorites</i>	<i>10</i>
<i>User Demonstrations</i>	<i>14</i>
<i>Origins and Formation</i>	<i>17</i>
<i>Technical Abstracts, May 19</i>	
<i>Systems and Languages</i>	<i>21</i>
<i>Web Applications and Mission Planning Software</i>	<i>23</i>
<i>Data Archive</i>	<i>26</i>
<i>Data Analysis and Concurrency</i>	<i>29</i>
<i>Science Abstracts, May 20</i>	
<i>Dynamics</i>	<i>32</i>
<i>Atmospheres</i>	<i>36</i>
<i>Space Physics</i>	<i>38</i>
<i>Terrestrial Planets and Titan</i>	<i>42</i>
<i>Craters and Impacts</i>	<i>46</i>
<i>Satellites</i>	<i>49</i>
<i>Keynote</i>	<i>52</i>

Asteroid Occultations: Video Techniques

J. McGaha*

Presenting and Corresponding Author: mcgaha@skepticus.com

Asteroid Occultations allow a direct measurement of the size and shape of an asteroid. Low light video taping permits high

precision timing and a record of the occultation. Video techniques and equipment will be discussed.

Enumeration of the Degenerates in the Solar Neighborhood

J. Holberg*

Presenting and Corresponding Author: holberg@vega.lpl.arizona.edu

The local population of white dwarf stars represents the "ground truth" sample for many statistical studies of white dwarf stars. Identifying and analyzing the complete white dwarf population within 20 parsecs of the sun provides an estimate of the number density and mass density of white dwarfs in our part of the galaxy. These studies can also provide useful information on such interesting and

useful details as the fraction of white dwarfs in binary systems and relative numbers of different white dwarf species. All of this information is fundamental to unraveling the history of star formation and evolution in our galaxy. I will report on results on recent work that helps better define the local white dwarf population and what has been learned.

Mars

May 19
10:15AM – 11:45AM

Chair: D. Choi

<i>Conference Schedule</i>	<i>II</i>
<i>Conference Welcome</i>	<i>VI</i>
<i>Science Abstracts, May 19</i>	
<i>Planetary Surfaces</i>	<i>1</i>
<i>Observation</i>	<i>4</i>
Mars	6
<i>Meteorites</i>	<i>10</i>
<i>User Demonstrations</i>	<i>14</i>
<i>Origins and Formation</i>	<i>17</i>
<i>Technical Abstracts, May 19</i>	
<i>Systems and Languages</i>	<i>21</i>
<i>Web Applications and Mission Planning Software</i>	<i>23</i>
<i>Data Archive</i>	<i>26</i>
<i>Data Analysis and Concurrency</i>	<i>29</i>
<i>Science Abstracts, May 20</i>	
<i>Dynamics</i>	<i>32</i>
<i>Atmospheres</i>	<i>36</i>
<i>Space Physics</i>	<i>38</i>
<i>Terrestrial Planets and Titan</i>	<i>42</i>
<i>Craters and Impacts</i>	<i>46</i>
<i>Satellites</i>	<i>49</i>
<i>Keynote</i>	<i>52</i>

Phoenix Payload Instruments

P. Woida*

Presenting and Corresponding Author: woida@lpl.arizona.edu

Introduction

On May 25th, 2008 the Phoenix Mars Scout Mission Robot will land in the Martian Arctic. Provided is a high level overview of the Phoenix Payload Instruments that will be used to search for water and to assess the habitability potential of the Vastitas Borealis region of Mars.

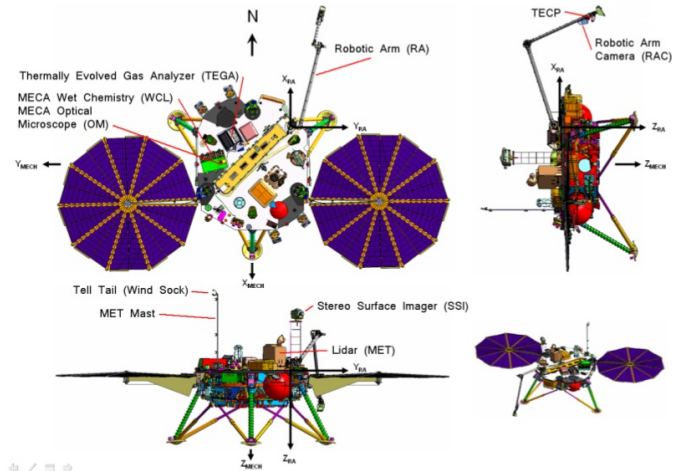


Figure 1. The Phoenix Mars Scout Mission Instrument Payload

HiRISE Observations of Fractured Mounds on Mars

C. Dundas* and A. McEwen

Presenting and Corresponding Author: colind@lpl.arizona.edu

Pingos are ice-cored hills, found in Arctic regions where near-surface groundwater freezes under pressure. As such, they provide useful information about near-surface ice and past water. Identification of pingos on Mars would provide useful information about the history of water and potentially offer clues to the formation of water-related features such as gullies. Pingos have previously been suggested on Mars, but the lower resolution of past orbital cameras has prevented identification of small-scale morphologies such as surface fracturing.

HiRISE has resolved fractured mounds on the Martian surface at several sites in the mid-latitudes, in a latitudinal band where gullies

are most abundant. In general, these features do not correspond with previously suggested pingos on Mars. However, they do resemble the morphologies of terrestrial pingos to varying degrees, most notably with the occurrence of resolvable surface fracturing. We have surveyed HiRISE data from several thousand orbits and found that fractured mounds on Mars are concentrated near 40° latitude in each hemisphere, suggestive of a water- or ice-related origin. These mounds fall into several broad categories based on morphology and setting, including some which are good analogues for terrestrial pingos. We will discuss the distribution, morphologies and settings of the observed mounds.

Enrichment of Argon over Mars' Winter Poles: Indicators of Peculiar Atmosphere Dynamics

W. Boynton* and A. Sprague

Presenting and Corresponding Author: wboynton@lpl.arizona.edu

Wet Chemistry Lab on Phoenix

S. Young*

Presenting and Corresponding Author: suzanne.young@tufts.edu

Production of Soils and the Shielding Effect of Small-Scale Surface Features

J. Moores*

Presenting and Corresponding Author: jmoores@lpl.arizona.edu

Invited Talk

Meteorites

May 19
1:00PM – 2:00PM

Chair: K. Kolb

<i>Conference Schedule</i>	II
<i>Conference Welcome</i>	VI
<i>Science Abstracts, May 19</i>	
<i>Planetary Surfaces</i>	1
<i>Observation</i>	4
<i>Mars</i>	6
Meteorites	10
<i>User Demonstrations</i>	14
<i>Origins and Formation</i>	17
<i>Technical Abstracts, May 19</i>	
<i>Systems and Languages</i>	21
<i>Web Applications and Mission Planning Software</i>	23
<i>Data Archive</i>	26
<i>Data Analysis and Concurrency</i>	29
<i>Science Abstracts, May 20</i>	
<i>Dynamics</i>	32
<i>Atmospheres</i>	36
<i>Space Physics</i>	38
<i>Terrestrial Planets and Titan</i>	42
<i>Craters and Impacts</i>	46
<i>Satellites</i>	49
<i>Keynote</i>	52

A Comprehensive Observational Survey of CR Chondrite Type-II Chondrules and Matrix

D. Schrader*, D. Lauretta, H. Connolly Jr.

Presenting and Corresponding Author: schrader@lpl.arizona.edu

Introduction

The Renazzo-like carbonaceous chondrites (CR) are among the most primitive material in the Solar System, and are therefore of primary importance for the study of early Solar System processes. CR chondrites have undergone aqueous alteration to varying degrees, ranging from minor to extreme, and therefore offer an excellent sample set to understand hydration of material in the early Solar System. As a result, the CRs are the focus of my PhD study. Through a comprehensive observational study of CR chondrites, we greatly advance our understanding of both the CR parent body, and minor body evolution and formation in the Solar System.

Background

The CR group was first recognized by [1], and then defined by [2]. Most of the chondrules are type-I (FeO-poor), as type-II chondrules (FeO-rich) are argued to be < 1 vol% of the chondrule population [2]. Among other minerals, they contain abundant Fe,Ni-rich metal and minor sulfides [2].

While most type-I chondrules in CR2s have been studied in some detail, type-II chondrules have been relatively ignored [3,4,5]. In our recent studies we observed that all type-II chondrules in CR2s contain sulfides, whereas type-I chondrules lack sulfides [6]. Since metal and sulfides respond more readily to their formation and alteration environments than silicates, they are important to study in order to further our understanding of primary and secondary formation processes. They also provide a unique geochemical signature of formation environment and mechanisms of CR meteorites.

Study

To decrease the sample bias, this survey will cover at least 17 separate CR meteorites (Table 1), which span a range of terrestrial residence age, discovery location on Earth (i.e. from the hot and cold deserts), and of pre and post terrestrial alteration. For the initial stage of my study, I use optical microscopy to understand the petrology of each polished thin section (PTS), then obtain X-Ray element maps of each PTS on the Cameca SX-50 electron microscope (EMP) at the UAz and compare the data with the petrography of the sample. X-Ray Maps assist in understanding the location and distribution of elements within each sample (Fig. 1). Immediate goals are measuring: the abundance, petrology, composition, and trends of opaques in type-II chondrules and matrix.

References

- [1] McSween H. Y. (1979) *Rev. Geophys. Space Phys.* 17, 1059-1078. [2] Weisberg M. K. et al. (1993) *GCA*, 57, 1567-1586. [3] Krot A. N. et al. (2002) *Meteorit. Planet. Sci.* 37, 1451-1490. [4] Connolly H.C. Jr. et al. (2003) *Lunar and Planet. Sci. XXXIV*, Lunar Planet. Inst., #1770 (abstr.). [5] Connolly H.C. Jr. et al. (2007) *Lunar and Planet. Sci. XXXVIII*, Lunar Planet. Inst., #1571 (abstr.). [6] Connolly H. C. Jr. et al. (2001) *Geochim. Cosmochim. Acta* 65, 4567-4588.

Table 1. CR Chondrites

Al Rais	LAP 04720
EET 87770	MAC 87320
EET 92011	MET 01017
EET 92042	MET 00426
EET 96259	NWA 801
GRA 95229	PCA 91082
GRA 98025	QUE 99177
GRO 95577	RBT 04133
GRO 03116	Renazzo
LAP 02342	Shiřr 033

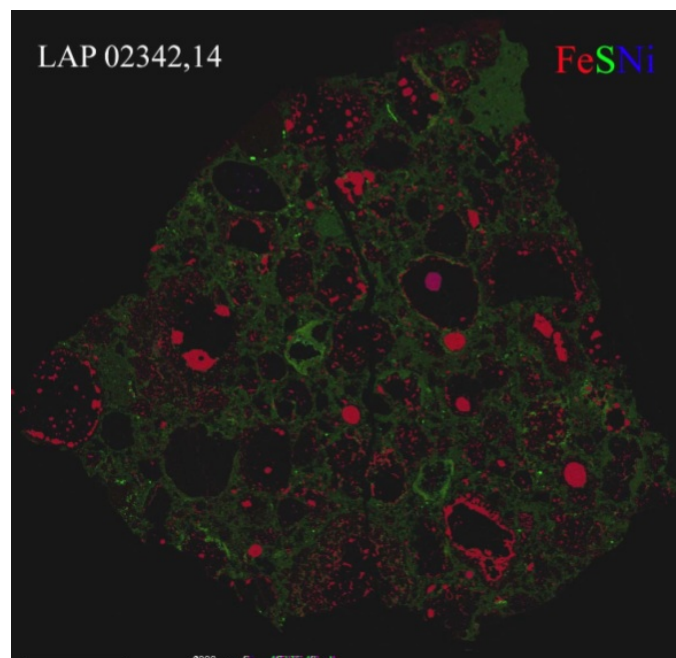


Figure 1. RGB X-Ray Map composite image with Fe on the red channel, S on the green, and Ni on the blue. Note the abundant S (green) in the matrix, and the lack of S in the majority of the chondrules.

Metal/Olivine Partitioning Experiments as an Aid to Defining the Cooling Rate of Pallasites

E. Hill*, K. Domanik, G. Huss, M. Drake

Presenting and Corresponding Author: eddy@lpl.arizona.edu

Pallasite meteorites are intimate mixtures of Mg-rich olivine ($(\text{Mg,Fe})_2\text{SiO}_4$) and FeNi alloy. Knowledge of the thermal histories of pallasites and of their position in their parent body is essential to understanding their origin and for the correct application of the clues they provide as to the composition and form of the bodies from which they originate. Several models have been proposed for their formation with the current favourite having pallasites as samples of the core-mantle boundary of disrupted asteroids or larger planetesimals [e.g., 1, 2, 3]. Other models propose they are samples of discrete metal pools found throughout the parent bodies [4], or that they originate near the surface as a result of melting and fractional crystallisation [5]. Their origin at the core-mantle boundary is supported, in part, by their metallographic determined cooling rate [3,4]. Study of Ni diffusion between kamacite ($\text{Fe}_{90-95}\text{Ni}_{10-5}$) and taenite ($\text{Fe}_{80-35}\text{Ni}_{20-65}$) crystals in the pallasite metal gives a cooling rate of ~ 1 °C/Ma for temperatures between 800 – 300 °C (the crystallisation temperature range for kamacite – taenite). Study of the major and minor chemistry of their olivines, however, suggests much higher cooling rates ($\sim 10^4$ °C/Ma) for temperatures >700 °C [e.g., 5, 6, 7]. These higher cooling rates are more inline with what we would expect for a near surface origin.

Pallasitic olivines have been described as chemically homogeneous in the major elements [3] but have chemical gradients in minor elements (e.g. Ca, Cr, Co, Ni) [e.g., 5,6,7]. It is assumed that these chemical profiles are the result of diffusion during slow cooling. Cooling at the metallographic derived rates, however, would result in homogeneous olivines. The rate of diffusion is in part dependent on the boundary condition i.e., the partition coefficient (D) at the metal-olivine interface. Attempts to fit olivine chemical profiles with a one-dimensional, spherical, cooling model [7] are hampered by a lack of minor element partitioning data. To date, only two D values suitable for use with the model are published [8].

Attempts to fit olivine chemical profiles using a constant boundary condition have been unsuccessful, suggesting that boundary conditions changed during cooling [7]. However, the lack of experimental data precludes modelling such changes. It is unlikely that Ds remained constant during pallasite formation because they depend on variables such as temperature (T), pressure (P), crystal and melt composition (X), and $f\text{O}_2$. The temperature, composition of the FeNi alloy and the $f\text{O}_2$ of the system are almost certain to have varied over time. Hence, metal/olivine Ds for a range of T, X and $f\text{O}_2$ are required to establish reliable, evolving boundary conditions that will allow us to better interpret the chemical profiles found in pallasitic olivines.

As a first approach to understanding how the boundary conditions change, we are performing experiments to determine the metal/olivine partition coefficients of Ni (D_{Ni}) and Co (D_{Co}). Experiments are being performed at decreasing temperatures and over a range of $f\text{O}_2$ and of alloy compositions. Our results to date show there is a clear increase in $\ln D_{\text{Ni}}$ (6.2 to 8.1) and $\ln D_{\text{Co}}$ (5.4 to 7.5) with decreasing $f\text{O}_2$ ($\log f\text{O}_2 = -8.86$ to -10.36). Since $\log f\text{O}_2$ decreases with decreasing temperature, we expect D_{Ni} and D_{Co} to increase as T decreases. Future experiments at lower temperatures will provide better controls on the shift in boundary conditions with decreasing T and shifting $f\text{O}_2$ and composition.

References: [1] Mason B. (1962) *Meteorites*, New York: Wiley, 274p. [2] Anders E. (1964) *Space Science Reviews* **3**, 583-714. [3] Buseck and Goldstein (1969) *Geol. Soc. Amer. Bull.* **80**, 2141-2158. [4] Wood, J.A. *Asteroids*, Univ. Ariz. Press. 849 – 891. [5] Miyamoto M. (1997) *J. Geo. Res.* **102**, 21613-21618. [6] Tomiyama and Huss (2005) *MAPS* **40**, A156. [7] Tomiyama and Huss (2006) *LPSC XXXVII* (2132). [8] Ehlers, Grove, Sisson, Recca and Zervas (1992) *Geochim. Cosmochim. Acta* **56**, 3733-3743.

MIL 05029: An L-Melt Rock From the Early Solar System

J. Weirich*

Presenting and Corresponding Author: jweirich@lpl.arizona.edu

The Ar-Ar technique can be used to date large impacts since the event creates enough heat to reset the chronometer. Most heavily shocked L chondrites have an Ar-Ar age of 500Ma, reflecting an impact at that time. However, the L-melt rock MIL05029 has an Ar-Ar age greater than 4500Ma, and no shock features since it is

a complete melt. Hence, an impact cannot be definitively identified. This meteorite also provides information about the source of K by ruling out pyroxene as a carrier, and providing evidence for 2 different grain sizes of the K host

Relationships Among Ungrouped Primitive Achondrites and Type-7 Ordinary Chondrites

K. Gardner-Vandy* and D. Lauretta

Presenting and Corresponding Author: kgardner@lpl.arizona.edu

An appreciable number of meteorites exist that have been classified as either ungrouped primitive achondrites or type 7 ordinary chondrites (OCs). We are studying the genesis of the FeO-rich primitive achondrites and brachinites, and a comparison of these meteorites to the highly metamorphosed and FeO-rich OCs is needed to fully understand the metamorphism and partial melting that occurred on FeO-rich parent bodies. However, a problem lies in the current classification scheme for the samples that have exceeded type-6 metamorphism but are not from fully

differentiated bodies. It does not effectively incorporate: 1) the type of heating undergone, 2) the peak temperature experienced, and 3) the precursor material. Here we compare the petrology and geochemistry of several of the meteorites currently classified as type 7 chondrites or primitive achondrites, and we assess whether or not these meteorites experienced a similar metamorphic history. We will also discuss a preliminary idea for an addition to the current classification scheme to incorporate these meteorites more effectively.

User Demonstrations

May 19
2:15PM – 3:15PM

Chair: C. Schaller

<i>Conference Schedule</i>	II
<i>Conference Welcome</i>	VI
<i>Science Abstracts, May 19</i>	
<i>Planetary Surfaces</i>	1
<i>Observation</i>	4
<i>Mars</i>	6
<i>Meteorites</i>	10
User Demonstrations	14
<i>Origins and Formation</i>	17
<i>Technical Abstracts, May 19</i>	
<i>Systems and Languages</i>	21
<i>Web Applications and Mission Planning Software</i>	23
<i>Data Archive</i>	26
<i>Data Analysis and Concurrency</i>	29
<i>Science Abstracts, May 20</i>	
<i>Dynamics</i>	32
<i>Atmospheres</i>	36
<i>Space Physics</i>	38
<i>Terrestrial Planets and Titan</i>	42
<i>Craters and Impacts</i>	46
<i>Satellites</i>	49
<i>Keynote</i>	52

Jbody User Demo

D. Lytle*

Presenting and Corresponding Author: dyer@lpl.arizona.edu

HiReport

G. McArthur*

Presenting and Corresponding Author: guym@arizona.edu

Obtaining, Using, and Understanding HiRISE Images

E. Eliason* and HiRISE Operations Team

Presenting and Corresponding Author: eeliason@pirl.lpl.arizona.edu

Introduction

The High Resolution Imaging Science Experiment (HiRISE), onboard the Mars Reconnaissance Orbiter (MRO) spacecraft, has been in near continuous science operations since November 2006 (<http://hirise.lpl.arizona.edu>). During this 19-month period, HiRISE has acquired more than 6,700 images covering about 960,000 square kilometers or about 0.67% of the Martian surface if it were all unique coverage. At 30-cm/pixel ground sampling, the HiRISE imaging offers the highest resolution orbital images ever obtained of the Martian surface. HiRISE red-filter imaging footprints are typically six kilometers cross-orbit and up to 36 kilometers in the down-orbit direction. For three-color imaging (blue-green, red, near-infrared filters) the cross-orbit coverage is 1.2 kilometers covering the middle 20% portion of a HiRISE observation. HiRISE observations can be enormous with image arrays sizes up to 20,048 x 120,000 pixels (2.4 gigapixels). Additionally, the data-storage requirements for housing the image collection are substantial with more than 33 terabytes currently needed for the collection.

Data Processing

Important tasks for the HiRISE operations team include processing the observational data to form scientifically useful image products, providing these data to its science team, and distributing the archive of science products to the general science community after the data have been validated. To make scientifically useful HiRISE products, processing pipelines have been developed to automate the production. The pipelines automatically retrieve observational data from the MRO project data base, perform radiometric calibration that will convert raw DN pixel values to radiometric units, perform geometric processing to remove optical distortion and transform the image to a standard map projection, and create images in

the JPEG2000 format along with product labels that describe the observational and map projection properties of the image.

Distributing Image Data

The distribution of HiRISE image products through the Internet can be a challenge with product sizes that often exceed three gigabytes and an archive larger than 33 terabytes. To meet this challenge, the HiRISE project has adopted the JPEG2000 Interactive Protocol (JPIP) technology, a proven method for efficiently distributing image data to the Internet community. The JPIP technology employs a client/server protocol for exchanging whole or parts of an image through a codestream of wavelet compression coefficients that are used by the client to render a raster image. Only those coefficients are transferred that are needed to render an image at the scale and dimension requested by the client. When rendering a new image, for example when zooming in on a sub-scene, only those additional coefficients are transferred and then combined with the coefficients already held by the client to generate the new image. The result is a rapid and efficient method for browsing, panning, and zooming through an image and minimizing the amount of data that is transferred over the Internet. The HiRISE team uses the IAS JPIP client/server software developed by the ITT Corporation.

Additional software tools are available for the display and analysis of HiRISE images. The HiRISE team uses the ISIS system developed by the USGS in Flagstaff Arizona to carry out data product generation and analysis. Additionally, many on the science team use the IDL/ENVI software package developed by the ITT Corporation. These and other tools will be demonstrated.

Origins and Formation

May 19
3:30PM – 4:30PM

Chair: K. Gardner-Vandy

<i>Conference Schedule</i>	II
<i>Conference Welcome</i>	VI
<i>Science Abstracts, May 19</i>	
<i>Planetary Surfaces</i>	1
<i>Observation</i>	4
<i>Mars</i>	6
<i>Meteorites</i>	10
<i>User Demonstrations</i>	14
Origins and Formation	17
<i>Technical Abstracts, May 19</i>	
<i>Systems and Languages</i>	21
<i>Web Applications and Mission Planning Software</i>	23
<i>Data Archive</i>	26
<i>Data Analysis and Concurrency</i>	29
<i>Science Abstracts, May 20</i>	
<i>Dynamics</i>	32
<i>Atmospheres</i>	36
<i>Space Physics</i>	38
<i>Terrestrial Planets and Titan</i>	42
<i>Craters and Impacts</i>	46
<i>Satellites</i>	49
<i>Keynote</i>	52

Adsorption as a Source of Water in the Inner Solar System: A Kinetic Monte Carlo Study

K. Muralidharan*, M. Stimpfl, P. Deymier, M. Drake
Presenting and Corresponding Author: krishna@u.arizona.edu

The origin of water in the inner solar system is not understood. It is believed that temperatures were too high in the accretion disk in the region of the terrestrial planets for hydrous phases to be thermodynamically stable. Thus, it has been postulated that water was delivered from beyond Mars by asteroidal or cometary material. However, isotopic and elemental ratios in comets and meteorites are inconsistent with this hypothesis. The accretion disk from which our planetary system formed was composed of solid grains bathed in a gas dominated by hydrogen, helium, and oxygen.

Some of that hydrogen and oxygen combined to make water vapor. Thus it is possible that water in the terrestrial planets is the result of adsorption of water onto grains in the inner solar system accretion disk. We examine this possibility quantitatively by exploring the adsorption dynamics of water molecules onto forsterite surfaces via kinetic Monte Carlo simulations. We conclude that many Earth oceans of water could be adsorbed, obviating the need for delivery of water from the outer solar system.

Photolytic Generation of Carbon Dioxide on Iapetus

E. Palmer* and R. Brown
Presenting and Corresponding Author: epalmer@lpl.arizona.edu

Cassini VIMS has detected Carbon Dioxide on Iapetus, a moon of Saturn where it is too hot for CO₂ to remain for much longer than a few hundred years. Since primordial CO₂ is unlikely, we explore the possibility of CO₂ being photolytically generated by solar UV

radiation. We have begun work using both a xenon and deuterium lamps as sources of UV light and have found photolytical reactions to be possible upon a mixture of carbon and water ice.

Problems with the Snowball Recovery Mechanism, Applications for Planetary Habitability.

A. Pavlov*, D. Noone, C. Cooper

Presenting and Corresponding Author: pavlov@lpl.arizona.edu

Early Earth was a warm planet despite the faintness of the young Sun. The standard explanation for this apparent paradox requires high atmospheric CO₂ levels in the Proterozoic-Archean so that the increased atmospheric greenhouse effect would compensate for the solar energy shortage. Accumulation of CO₂ in the atmosphere was also proposed as the mechanism of recovery from the most severe glaciations in the earth history – Snowball glaciations.

I found that under the decreased solar luminosity even at moderate CO₂ levels, the polar surface temperatures could drop below the CO₂ condensation temperatures. If CO₂ were condensing at the surface it could not have stabilized climate against climate perturbations by means of the carbonate-

silicate cycle or could not have accumulated in the atmosphere during Snowball events. My climate simulations suggest that some additional warming was required throughout Archean and Proterozoic to prevent CO₂ from condensing.

Carbonate-silicate cycle and the elevated atmospheric CO₂ levels are also suggested as the mechanism to extend the outer edge of the habitable zone – the shell of space around a star where surface temperatures are high enough to maintain liquid water on a planetary surface. Because of the CO₂ condensation in the polar regions, the habitable zone for the water-rich planets around solar-like stars could be significantly narrower than we previously thought.

Low-Temperature Sulfides in Stardust: TEM Analysis of a Sphalerite/Pyrrhotite Assemblage from Track 7

E. Berger*, L. Keller, D. Joswiak, G. Matrajt, D. Lauretta
Presenting and Corresponding Author: elberger@lpl.arizona.edu

Introduction: Stardust achieved its mission goal of catching comet and interstellar dust particles and returning them to Earth for analysis. The particles collected span a wide range of compositions, each of which yields information about the comet's history. The refractory components in this collection reveal the large-scale distribution of high-temperature components in the early Solar System. Studies of sulfides complement this information by revealing the low-T processes, as well as minor element mobilization recorded in these samples. We investigate a terminal particle from track 7, which has co-existing minerals from the Fe-Ni-S and Fe-Zn-S systems.

Results & Discussion: A microtomed section of a Stardust particle from track 7 (T7, 10, 85) was analyzed via TEM at JSC and at the University of Washington. The particle is polycrystalline and is predominately Ni-free pyrrhotite that shows distinct superstructure reflections in electron diffraction patterns. The particle also contains a μm -sized grain of Ni-bearing pyrrhotite $[(\text{Fe}_{0.93}\text{Ni}_{0.07})_{1-x}\text{S}]$ showing the same superstructure reflections, and a μm -sized grain of Fe-rich sphalerite (Zn,Fe)S. The sphalerite contains minor Mn (<2 at.%) and shows fine-scale twinning on (111). The sphalerite and Ni-bearing pyrrhotite are not in direct contact.

The pyrrhotite superstructure reflections are only stable below ~ 340 °C [1]. If the grain were heated above this temperature, the superstructure reflections can be recovered only through slow cooling. The persistence of these reflections indicates that the pyrrhotite did not experience high temperatures during aerogel capture.

If sphalerite and pyrrhotite are in equilibrium then the wt% Fe in the sphalerite constrains temperature and sulfur fugacity of their formation [2]. Using the temperature 340 °C yields a value for $\log f_{\text{S}_2}$ of -34. However, sphalerite and pyrrhotite can not co-exist under these conditions in equilibrium [3]. We conclude that these minerals are not equilibrated.

Many of Stardust Fe-Ni sulfides contain <2 at.% Ni (except pentlandite). This range matches sulfide compositions in anhydrous IDPs [4]. The increased Ni-content in a portion of this pyrrhotite, as well as the disequilibrium between the pyrrhotite and sphalerite, indicates that this grain has experienced processing, and may be more similar to hydrous IDPs or chondritic samples. One possibility is that Ni- and Zn-bearing pyrrhotite formed in the nebula. The Ni and Zn may have subsequently migrated during solid state thermal metamorphism. A second possibility is precipitation of pyrrhotite during parent-body aqueous alteration followed by Ni and Zn precipitation at a later time. Either case suggests that the grain had to remain at relatively low temperatures (<340 °C) during either nebular transport to Wild 2 or parent body alteration within Wild 2.

References: [1] Li F. et al. 1996. *Journal of Solid State Chemistry* 124: 264-271. [2] Scott S. D. and Barnes H. L. 1971. *Economic Geology* 66: 653-669. [3] Scott S. D. and Barnes H. L. 1972. *Geochimica et Cosmochimica Acta* 36: 1275-1295. [4] Zolensky et al. 2006. *Science* 314: 1735-1739.

Systems and Languages

May 19
9:00AM – 10:30AM

Chair: C. Schaller

<i>Conference Schedule</i>	II
<i>Conference Welcome</i>	VI
<i>Science Abstracts, May 19</i>	
<i>Planetary Surfaces</i>	1
<i>Observation</i>	4
<i>Mars</i>	6
<i>Meteorites</i>	10
<i>User Demonstrations</i>	14
<i>Origins and Formation</i>	17
<i>Technical Abstracts, May 19</i>	
Systems and Languages	21
<i>Web Applications and Mission Planning Software</i>	23
<i>Data Archive</i>	26
<i>Data Analysis and Concurrency</i>	29
<i>Science Abstracts, May 20</i>	
<i>Dynamics</i>	32
<i>Atmospheres</i>	36
<i>Space Physics</i>	38
<i>Terrestrial Planets and Titan</i>	42
<i>Craters and Impacts</i>	46
<i>Satellites</i>	49
<i>Keynote</i>	52

DNS – A Glue of the Internet and Much More

T. Spriggs*

Presenting and Corresponding Author: tims@uahirise.org

The Internet Domain Name System (DNS) allows computers to resolve names to addresses as well as a wealth of other information. While many people are aware that DNS can take a name like "hindmost.lpl.arizona.edu." and return an A record with "150.135.111.1", they may not be aware that other more varied kinds of information can be stored or transmitted in this

globally accessible database. Since its creation in 1983, DNS has become the de-facto standard for storing a very large and dynamic set of information in a distributed tree structure. This information commonly includes IP addresses, mail hosts, geographic coordinates, service locations, public keys, arbitrary files and even IP.

Massive Storage on the Cheap

J. Plassmann*, D. Jones, T. Spriggs, T. Forrester

Presenting and Corresponding Author: joep@arizona.edu

Recent advances in storage systems, networking, and Open Source software should made it possible to cobble together massive storage arrays capable of managing hundreds of Terabytes of information at a very low cost/TB. However, the same old problems of managing array performance, data reliability, redundancy, replication and backup continue to

be major issues. I plan to discuss a few approaches the HiROC systems group is looking at to tackle this issue with our real-life problem: the massive amount of HiRISE data that has already broken all original storage projections and has strained the the HiRISE operations budget to manage it.

Secure Client-Server Authentication in Java

A. Davidson*

Presenting and Corresponding Author: andrewd@email.arizona.edu

As the already ubiquitous client-server model of computing finds a place in an ever increasing number of venues, the need for secure methods of authentication grows. At the heart of the issue of authentication is the need for a secure server to gather private credentials over a potentially insecure network. This talk briefly summarizes an asymmetric encryption

and decryption system build entirely upon the Java Foundation Classes and the Java Security package. This system remains secure even if all communication between client and server is intercepted. If time permits, there will also be a high-level discussion of the underlying DSA protocol used to implement the authentication system.

Web Applications and Mission Planning Software

**May 19
10:45AM – 11:30AM**

Chair: C. Schaller

<i>Conference Schedule</i>	<i>II</i>
<i>Conference Welcome</i>	<i>VI</i>
<i>Science Abstracts, May 19</i>	
<i>Planetary Surfaces</i>	<i>1</i>
<i>Observation</i>	<i>4</i>
<i>Mars</i>	<i>6</i>
<i>Meteorites</i>	<i>10</i>
<i>User Demonstrations</i>	<i>14</i>
<i>Origins and Formation</i>	<i>17</i>
<i>Technical Abstracts, May 19</i>	
<i>Systems and Languages</i>	<i>21</i>
Web Applications and Mission Planning Software	23
<i>Data Archive</i>	<i>26</i>
<i>Data Analysis and Concurrency</i>	<i>29</i>
<i>Science Abstracts, May 20</i>	
<i>Dynamics</i>	<i>32</i>
<i>Atmospheres</i>	<i>36</i>
<i>Space Physics</i>	<i>38</i>
<i>Terrestrial Planets and Titan</i>	<i>42</i>
<i>Craters and Impacts</i>	<i>46</i>
<i>Satellites</i>	<i>49</i>
<i>Keynote</i>	<i>52</i>

Reusability in Web Applications

G. McArthur*

Presenting and Corresponding Author: guym@arizona.edu

Well-designed web applications should promote re-use as much if not more than ordinary applications. I will show design

patterns and best practices that enable re-use from web applications, both at the code level and the external interface or service level.

Load Testing the Web Application Stack: How do you Know your Web Application can Handle the Load?

R. Heyd*

Presenting and Corresponding Author: rod@pirl.lpl.arizona.edu

Many NASA and NSF funded science programs are increasingly using web sites and web applications as part of their overall public outreach programs. Some of these sites have a relatively high profile, and will often see large spikes in usage just after a big press release has been made.

The HiRISE team has already created a popular website for viewing images of Mars taken with the HiRISE camera, and an online

application to allow the public at large to suggest targets is in development. However, without proper load testing of these applications, it is impossible to say how well these applications will work under a heavy load spike. This talk will focus on experiences gained from load testing a java servlet that will eventually act as the interface between the public application software and the HiRISE targeting database.

Extending JMARS for HiRISE Science Planning and Beyond

C. Schaller*

Presenting and Corresponding Author: schaller@pirl.lpl.arizona.edu

JMARS (Java Mission-planning and Analysis for Remote Sensing)[1] is a geographic information system application created at the Mars Space Flight Facility at ASU for Mars Odyssey mission planning and for Mars science data analysis. It provides a visual, layered approach to displaying multiple geospatial data sets simultaneously, including global image maps, regional mosaics, single-image “stamps,” polygonal data sets such as ESRI shape files, and gridded numeric data sets.

Its use as a mission planning tool has been extended to Mars Reconnaissance Orbiter science planning via an MRO planning layer, which provides a generic means of planning an observation for an MRO science instrument. The HiRISE software developers and the JMARS developers have further extended the tool to HiRISE-specific planning through a custom instrument parameter editor linked to the MRO planning layer (Figure 1). We designed the software interface to the planning layer to be generic, so that any of the MRO science instrument teams can use the same interface for their own custom editors.

In addition to the instrument parameter editor, we have extended the mechanism JMARS uses for drawing generic MRO instrument observation footprints. Through an additional instrument-generic interface, we can draw the individual HiRISE CCD footprints inside the generic instrument footprint, providing our science planners with a detailed view of the target as HiRISE will observe it. We use this same interface to draw targeting crosshairs in the generic footprint, enabling more precise planning.

Finally, we have extended the polygonal shape layer through pre-existing interfaces to draw outlines for HiRISE observation suggestions, planned observations, and already acquired observations.

The abstraction provided by these interfaces allows us to use our own HiRISE-specific database,

for example, without exposing its details unnecessarily: The polygonal shape layer is not aware of how HiRISE suggestions are stored, or even what particular sets of metadata are available for the different polygonal sources. Likewise, the MRO planning layer is not aware of the specifics of HiRISE instrument commanding or the details of determining a particular CCD’s footprint within the larger generic observation footprint. Existing interfaces even allow a developer to create a completely new layer adapted to whatever purpose is needed, including new spacecraft missions.

Limitations: JMARS source code is not currently available to the general public, but plans for opening it up are in development (E. Engle, JMARS principal engineer, personal communication). Furthermore, JMARS is currently limited to Mars science; the underlying geospatial model assumes Mars planetary dimensions. The tool is being adapted for Lunar Reconnaissance Orbiter planning, however, so it is likely to be able to be adapted to any roughly spherical planetary body.

Availability: JMARS is freely available for download from the ASU JMARS website at <http://jmars.asu.edu>.

References: [1] Gorelick N. S. et al., (2003) LPS XXXIV, Abstract 2057.

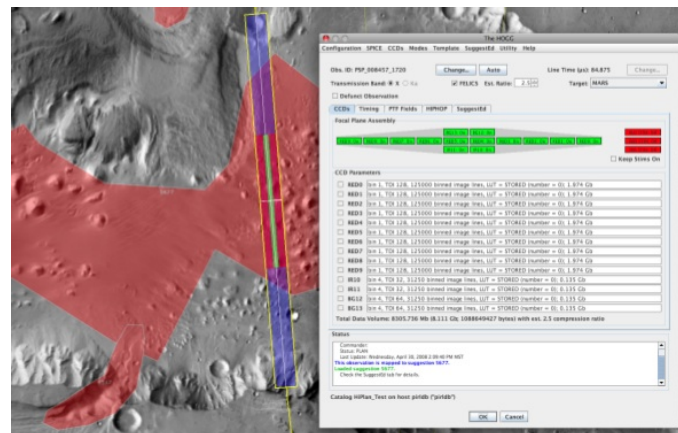


Figure 1: JMARS extended for HiRISE science planning.

Data Archive

May 19
12:30PM – 1:00PM

Chair: C. Schaller

<i>Conference Schedule</i>	II
<i>Conference Welcome</i>	VI
<i>Science Abstracts, May 19</i>	
<i>Planetary Surfaces</i>	1
<i>Observation</i>	4
<i>Mars</i>	6
<i>Meteorites</i>	10
<i>User Demonstrations</i>	14
<i>Origins and Formation</i>	17
<i>Technical Abstracts, May 19</i>	
<i>Systems and Languages</i>	21
<i>Web Applications and Mission Planning Software</i>	23
Data Archive	26
<i>Data Analysis and Concurrency</i>	29
<i>Science Abstracts, May 20</i>	
<i>Dynamics</i>	32
<i>Atmospheres</i>	36
<i>Space Physics</i>	38
<i>Terrestrial Planets and Titan</i>	42
<i>Craters and Impacts</i>	46
<i>Satellites</i>	49
<i>Keynote</i>	52

Managing Versions of Science Data Products Using Databases and Software Tools

R. Heyd*

Presenting and Corresponding Author: rod@pirl.lpl.arizona.edu

A big problem facing projects with large data processing needs is managing and tracking versions of products. In addition, determining what products need to be versioned can also be a surprisingly complicated problem.

In the specific case of HiRISE, updated versions of science products need to be created for many different reasons. Management of the creation of these products

and tracking them through our processing system to eventual public release is a basic need of our processing pipelines. This presentation will examine several approaches to product versioning that the HiRISE Ground Data Systems team evaluated and present the final scheme which manages the production of product versions via a small software application and metadata stored within the HiRISE database system.

PDS_JP2

B. Castalia*, A. Davidson, B. Pearson

Presenting and Corresponding Author: castalia@arizona.edu

The PDS_JP2 software provides applications and a library of reusable C++ classes for the conversion between PDS uncompressed image data files with an attached metadata label and a compressed JP2 image data file with a detached PDS metadata label file. This software was developed for the production of HiRISE (<http://hirise.lpl.arizona.edu/>) observation RDR data products in PDS/JP2 file format. The software can include in the JP2 file a GeoTIFF box that provides georeferencing information.

PDS file formats:

PDS/JP2 is a new Planetary Data System (<http://pds.jpl.nasa.gov/>) standard for delivery, archiving and distribution of image data. It was established in response to the need to manage large image data files.

The conventional PDS flat image file format includes a text label containing metadata that characterizes the image; the image data typically follows the label in the same file as binary pixel values. The PDS/JP2 format also provides a text metadata label that conforms to pre-existing PDS standards. The label is in a separate file from the image data that is stored in ISO JPEG2000 (<http://www.jpeg.org/jpeg2000/>) format using this standard's JP2 file structure. The JP2 structure includes a set of required data boxes that describe the organization of the loss-lessly compressed image codestream (based on a discreet wavelet transform, DWT) contained in its own data box.

For PDS/JP2 files an optional JP2 data box is used to provide a relative file URL to the label file along with a data provider signature. The HiRISE RDR data products use another optional data box to include GeoTIFF (<http://www.remotesensing.org/geotiff/geotiff.html>) georeferencing information derived from the label metadata. GeoTIFF has been established by remote sensing, GIS and cartographic organizations and is supported by several commercial and open source software packages used in spatial data processing.

A key feature of the JPEG2000 codestream is that any selected area of the image may be decompressed without having to process the entire file. In addition, the DWT data coding technique enables the image data to be decompressed at a selected resolution level. In effect, the JPEG2000

codestream can contain an implicit image

PDS_JP2 programs:

The PDS_to_JP2 program is used to convert conventional PDS flat image files to PDS/JP2 formatted files. The program does automatic label manager selection to handle product-specific conversion requirements with fallback to a generic conversion manager. The JP2 file is generated with control of all configurable aspects of loss-less JPEG2000 compression and metadata content in the generated JP2 file, with reasonable defaults for all specifications. A data provider signature may be included with the reference to the external label file. Inclusion of a GeoTIFF box in the JP2 file is an option.

The JP2_to_PDS application is used to convert PDS/JP2 formatted files to conventional PDS flat image files. Like PDS_to_JP2, an appropriate label manager is automatically selected to handle the label conversion. By default all of the image data is decompressed at full resolution, but any image area may be selected for decompression at any resolution level provided by the JP2 file. The image description in the label is kept consistent with however the image data is rendered. Selective image rendering is particularly useful when only a particular region or low resolution presentation rendering is of interest or when working with the entire uncompressed image would be difficult or, for some computer systems, impossible. The raw image data is suitable for importing into various image analysis applications.

Class library:

The PDS_JP2 software package includes a library of C++ classes on which the application programs are built. These classes include PDS label management and image data JP2 file encoding and decoding management. The library may be used to build new applications and/or extended to provide additional capabilities. The label managers employ the idaeim PVL library (<http://pirl.lpl.arizona.edu/software/idaeim/PVL/>). The JP2 encoders and decoders employ the Kakadu Software (<http://www.kakadusoftware.com/>) library.

The PDS_JP2 package is open software available from http://hirise.lpl.arizona.edu/tools/pds_jp2.php.

Data Analysis and Concurrency

**May 19
1:00PM – 1:40PM**

Chair: C. Schaller

<i>Conference Schedule</i>	<i>II</i>
<i>Conference Welcome</i>	<i>VI</i>
<i>Science Abstracts, May 19</i>	
<i>Planetary Surfaces</i>	<i>1</i>
<i>Observation</i>	<i>4</i>
<i>Mars</i>	<i>6</i>
<i>Meteorites</i>	<i>10</i>
<i>User Demonstrations</i>	<i>14</i>
<i>Origins and Formation</i>	<i>17</i>
<i>Technical Abstracts, May 19</i>	
<i>Systems and Languages</i>	<i>21</i>
<i>Web Applications and Mission Planning Software</i>	<i>23</i>
<i>Data Archive</i>	<i>26</i>
Data Analysis and Concurrency	29
<i>Science Abstracts, May 20</i>	
<i>Dynamics</i>	<i>32</i>
<i>Atmospheres</i>	<i>36</i>
<i>Space Physics</i>	<i>38</i>
<i>Terrestrial Planets and Titan</i>	<i>42</i>
<i>Craters and Impacts</i>	<i>46</i>
<i>Satellites</i>	<i>49</i>
<i>Keynote</i>	<i>52</i>

Jbody: A Planetary Body Data Analysis Tool

D. Lytle*, V. Pasek, J. Ivens, R. Watson

Presenting and Corresponding Author: dyer@lpl.arizona.edu

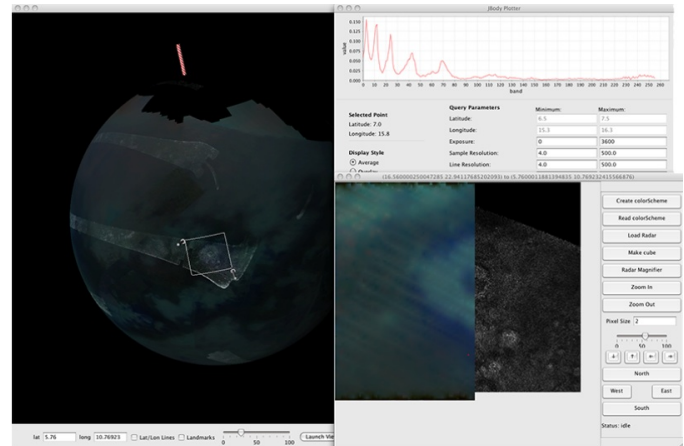
JBody will allow scientists to move easily from the global perspective of a planetary body to a specific region of interest.

Multi-instrument data overlay is an integral part of science analysis. JBody facilitates this aspect of investigation by allowing the user to dynamically generate maps of specific regions from multiple datasets.

Currently, JBody is in development and will be used by the VIMS Science Team. A future version of the software will be generalized to other planetary bodies and other instruments.

The Java platform and Java 3D are used for this project. They are open source,

contain most of the needed tools, are easily portable across multiple platforms, and have excellent IDEs available.



Stage_Manager

B. Castalia* and A. Davidson

Presenting and Corresponding Author: castalia@arizona.edu

The Stage_Manager software is designed to support remote management and monitoring capabilities for Conductor pipeline processing applications. The design of the system is based on a multithreaded, asynchronous, message passing system.

The Stage_Manager enables clients from any system, local or remote, to make a connection on a designated system port which is used to establish two-way socket communication channels. Each communication channel is managed by a pair of Messengers, one on each end of the channel. The Stage_Manager is capable of authenticating each client connection using an asymmetric public-private key pair mechanism.

A Messenger can send a Message across the communication channel and receive Messages that are sent. Messages may be received synchronously under the control of the Messenger employer or the Messenger can be told to listen asynchronously for Messages which will be autonomously routed for delivery. If the communication channel becomes unusable the employer is provided with a notification Message of this event. A Messenger can be provided with the forwarding address of one or more other Messengers to whom an autonomously received Message may be sent rather than being delivered directly to the employer.

A Message is formatted in plain ASCII text using the ISO standard Parameter Value Language (PVL). Each Message contains a message start synchronization pattern to enable recovery from a corrupted data stream in the communication channel. Each Message also includes routing information that specifies the addresses of destination Messengers to convey the Message as well as receipt routing that can be used send a reply to any Message. When a Message is autonomously received the destination routing information is examined

to determine whether the Message should be delivered to the employer or forwarded to another Messenger. Messages with unknown routing addresses are returned to the sender after being marked as undeliverable.

The Stage_Manager system uses a parameter naming protocol to convey information to clients about other connected clients and establish Message forwarding connections between Messengers. Thus Stage_Manager clients may send Messages to the Stage_Manager or any other client of the Stage_Manager.

Remote Conductor management and monitoring is enabled by having each Conductor establish a connection with the Stage_Manager on its host system using an implementation of the Conductor Management interface, layered on top of a Messenger, that translates Messages, using an appropriate PVL protocol, to corresponding interface method calls on the Conductor. A corresponding remote Conductor Management object makes a connection through the Stage_Manager on the selected host system to a selected Conductor and sends and receives the appropriate protocol Messages to implement the interface methods. In this way the same Conductor Manager GUI object can be used directly with a Conductor object as a single application, or remotely through the Stage_Manager Messenger system as a client-server application. When a Conductor is running its pipeline processing operations sends notices of processing events and/or process log stream output through its Management interface. It receives notices from its Management interface that control its processing operations and the sending of processing event notices and log stream.

The Stage_Manager and Messenger software is implemented as pure Java classes.

Dynamics

May 20
9:00AM – 10:00AM

Chair: E. Berger

<i>Conference Schedule</i>	II
<i>Conference Welcome</i>	VI
<i>Science Abstracts, May 19</i>	
<i>Planetary Surfaces</i>	1
<i>Observation</i>	4
<i>Mars</i>	6
<i>Meteorites</i>	10
<i>User Demonstrations</i>	14
<i>Origins and Formation</i>	17
<i>Technical Abstracts, May 19</i>	
<i>Systems and Languages</i>	21
<i>Web Applications and Mission Planning Software</i>	23
<i>Data Archive</i>	26
<i>Data Analysis and Concurrency</i>	29
<i>Science Abstracts, May 20</i>	
Dynamics	32
<i>Atmospheres</i>	36
<i>Space Physics</i>	38
<i>Terrestrial Planets and Titan</i>	42
<i>Craters and Impacts</i>	46
<i>Satellites</i>	49
<i>Keynote</i>	52

Possible Discrepancy in the Number Distribution of Asteroids in the Main Belt

D. Minton* and R. Malhotra

Presenting and Corresponding Author: daminton@lpl.arizona.edu

Introduction: We present here evidence for a possible depletion pattern observed in the population of $D > 50$ km asteroids in the Main Asteroid Belt that is consistent with a sweeping of both jovian mean motion resonances and the v_6 secular resonance. Using an analytical model of the sweeping v_6 resonance, this depletion pattern can be used to estimate rate of migration of Saturn, and hence provide a constraint on the duration of asteroidal bombardment during the LHB.

Evidence for a depletion pattern: We have restricted our study to asteroids with diameters $D > 50$ km. The Yarkovsky effect is not effective for large asteroids [cf., 1], so the only forces that have perturbed large asteroids over the solar system's history are gravitational and collisional. It has been estimated that the creation and destruction lifetimes of 50 km asteroids are ~ 20 Gy and ~ 4 Gy, respectively [2]. Therefore we assume that the population of asteroids with $D > 50$ km has not undergone appreciable collisional evolution since the end of the LHB. This population is also thought to be observationally complete [3].

We compare the distribution of observed $D > 50$ km asteroids against a simulated asteroid belt obtained by numerically integrating a hypothetical distribution of asteroids generated by filling up the main asteroid belt region with a uniform distribution of test particles. The test particles are numerically integrated along with all the planets, and the planets interact with each other and perturb the test particles, but the test particles have no effect on the planets. The test particles are considered lost if they pass within 1 Hill radius of a planet. The simulation

was ended after 100 My, and the particles were binned into 0.05 AU proper semimajor axis bins. The bin-by-bin particle loss history was used to extrapolate the size of the bin at 4 Gy. The extrapolated bin size was compared with the observed $D > 50$ km asteroids in the Main Belt where a "percent discrepancy" is defined as

$$\text{Discrepancy \%} = \frac{N_{\text{sim}} - N_{\text{obs}}}{N_{\text{obs}}} \times 100$$

The results are shown in Fig. 1.

References:

- [1] Farinella P. et al. (1998) *Icarus*, 132, 378–387. [2] Cheng A.F. (2004) *Icarus*, 169, 357–372. [3] Jedicke R. et al. (2002) *Asteroids III*, 71–87.

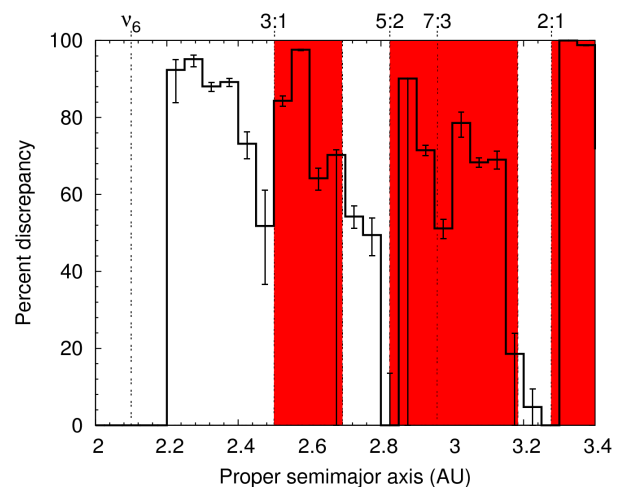


Figure 1: Depletion pattern observed in the Main Asteroid Belt. The shaded regions are regions that would have been swept by jovian mean motion resonances (MMR) in a -0.4 AU migration of Jupiter. The non-MMR component explained by Saturn's migration of at least 0.8 AU with a monotonically declining sweep rate.

OGLE-2006-BLG-109L: A Solar System Look-alike

R. Malhotra* and D. Minton

Presenting and Corresponding Author: renu@lpl.arizona.edu

The extrasolar system OGLE-2006-BLG-109L is the first multiple-planet system to be discovered by gravitational microlensing (Gaudi et al., 2008). This system has been described as an analog for our own solar system because the two large planets that have been detected have mass ratios, semimajor axis ratios, and equilibrium temperatures that are similar to those of Jupiter and Saturn, although the system is more compact than our own because the mass of the star is only 0.5 solar mass. The detailed orbital parameters of the two planets are not well constrained, but our dynamical stability considerations suggest that the orbits may be of low eccentricity. The mutual gravitational perturbations of the planets excite small orbital eccentricities of a few percent, not dissimilar to

those of our own Jupiter and Saturn. However, in the habitable zone of the host star, these two planets resonantly excite large orbital eccentricities on an earth-mass planet; this effect would drive such a planet out of the habitable zone for a substantial fraction of its orbital period, jeopardizing its habitability. We show that an additional inner planet of $\sim >0.3$ earth-mass at $< \sim 0.1$ AU would suppress the eccentricity perturbation and greatly improve the prospects for habitability of the system. Thus, the planetary architecture of a potentially habitable OGLE-2006-BLG-109L planetary system -- with two "terrestrial" planets and two jovian planets -- could bear even closer resemblance to our own Solar system than suggested by the two detected planets alone.

In the Groove: Mean Motion Resonances between Centaurs and the Giant Planets

B. Bailey* and R. Malhotra

Presenting and Corresponding Author: bbailey@math.arizona.edu

The Centaurs are a transient population of small bodies between the orbits of Jupiter and Neptune. Their orbits exhibit chaotic behavior due to frequent close encounters with the giant planets. Time series plots of the osculating orbital elements of each known Centaur during a 30 million year numerical integration show a rich variety of dynamical behavior. A subset of these Centaurs spend periods of time at constant semimajor axis, suggesting that they are trapped in a mean motion resonance with one of the giant planets

during those periods. We have identified and tested the possible resonances for each case. In the majority of cases, the orbital periods of the Centaur and one of the planets are in a small whole-number ratio and the calculated resonance angle librates with restricted amplitude, confirming that these are indeed mean motion resonances. The Centaur 2005 TH173 is an interesting exception: it remains in a quasi-stable orbit for the entire numerical integration, but it is not in a mean motion resonance with any of the giant planets.

The Problem of Producing High-Perihelion Kuiper Belt Objects

K. Volk*

Presenting and Corresponding Author: kvolk@lpl.arizona.edu

The Kuiper belt can be divided into many distinct dynamical classes including the classical belt, the resonant population, the scattered disk, and a group of high-perihelion objects referred to as detached objects or the extended scattered disk. The dynamics of the first three classes is well understood in the context of interactions with the giant planets, but the last class is quite puzzling. These detached objects are characterized by having semi-major axes above 50 AU with perihelia larger than about 40 AU. Such large perihelia

put these objects out of the reach of gravitational encounters with Neptune, which means that mechanisms other than gravitational encounters must be invoked to explain their current orbits. Resonant interactions with the giant planets can sometimes raise an object's perihelion to above 40 AU, but the process is inefficient and fails to reproduce observed objects with very large perihelia, such as Sedna ($q = 75$ AU). I will review this problem and outline some current investigations into its solution.

Atmospheres

May 20
10:00AM – 10:30AM

Chair: E. Berger

<i>Conference Schedule</i>	II
<i>Conference Welcome</i>	VI
<i>Science Abstracts, May 19</i>	
<i>Planetary Surfaces</i>	1
<i>Observation</i>	4
<i>Mars</i>	6
<i>Meteorites</i>	10
<i>User Demonstrations</i>	14
<i>Origins and Formation</i>	17
<i>Technical Abstracts, May 19</i>	
<i>Systems and Languages</i>	21
<i>Web Applications and Mission Planning Software</i>	23
<i>Data Archive</i>	26
<i>Data Analysis and Concurrency</i>	29
<i>Science Abstracts, May 20</i>	
<i>Dynamics</i>	32
Atmospheres	36
<i>Space Physics</i>	38
<i>Terrestrial Planets and Titan</i>	42
<i>Craters and Impacts</i>	46
<i>Satellites</i>	49
<i>Keynote</i>	52

Assessment of Saturn's Atmosphere and Zonal Winds from Cassini/VIMS

D. Choi*, A. Showman, R. Brown

Presenting and Corresponding Author: dchoi@lpl.arizona.edu

The Cassini spacecraft, currently orbiting Saturn, has returned a wealth of data on the planet and its satellites. As part of its suite of scientific instruments, the Visual and Infrared Mapping Spectrometer (VIMS) is capable of taking near-simultaneous observations in a wide visible and near-infrared spectral window of a target. In particular, the spectral region around 5 microns is particularly interesting, because at this wavelength, clouds and other features of Saturn's atmosphere can be seen "backlit" against Saturn's thermal

emission. I will discuss our continuing analysis of VIMS data about Saturn's atmosphere and discuss the morphology, latitudinal distribution, and other properties of the observed features. I will also discuss our measurements of the latitudinal zonal wind profile that we have constructed by modifying our automated cloud feature tracking technique to the VIMS datasets. The implications of our results about the state of Saturn's atmosphere will be explored.

The Origin of Oxygen Species in Titan's Atmosphere

S. Hörst*, V. Vuitton, R. Yelle

Presenting and Corresponding Author: horst@lpl.arizona.edu

The detection of O^+ precipitating into Titan's atmosphere by the Cassini Plasma Spectrometer (CAPS) (Hartle et al. 2006) represents the discovery of a previously unknown source of oxygen in Titan's atmosphere. The photochemical model presented here shows that those oxygen ions are incorporated into CO and CO_2 . We show that the observed abundances of CO, CO_2 and H_2O can be simultaneously reproduced using

an oxygen flux consistent with the CAPS observations (Hartle et al. 2006) and an OH flux consistent with predicted production from micrometeorite ablation (English et al. 1996). It is therefore unnecessary to assume that the observed CO abundance is the remnant of a larger primordial CO abundance or to invoke outgassing of CO from Titan's interior as a source of CO.

Space Physics

May 20
10:45AM – 12:00AM

Chair: K. Volk

<i>Conference Schedule</i>	II
<i>Conference Welcome</i>	VI
<i>Science Abstracts, May 19</i>	
<i>Planetary Surfaces</i>	1
<i>Observation</i>	4
<i>Mars</i>	6
<i>Meteorites</i>	10
<i>User Demonstrations</i>	14
<i>Origins and Formation</i>	17
<i>Technical Abstracts, May 19</i>	
<i>Systems and Languages</i>	21
<i>Web Applications and Mission Planning Software</i>	23
<i>Data Archive</i>	26
<i>Data Analysis and Concurrency</i>	29
<i>Science Abstracts, May 20</i>	
<i>Dynamics</i>	32
<i>Atmospheres</i>	36
Space Physics	38
<i>Terrestrial Planets and Titan</i>	42
<i>Craters and Impacts</i>	46
<i>Satellites</i>	49
<i>Keynote</i>	52

Examining Solar Energetic Particle Diffusion through Dropout Observations

E. Chollet* and J. Giacalone

Presenting and Corresponding Author: echollet@lpl.arizona.edu

We present a new observational constraint on the energetic particle diffusion coefficient ratio in the solar wind using ACE/ULEIS and Wind/STEP energetic ion data. $\kappa_{\perp}/\kappa_{\parallel}$ (the ratio of cross-field diffusion to diffusion along magnetic field lines) is an important parameter in space physics research, determining, among other things, how efficiently particles can be transported to high heliographic latitudes. Energetic particle flux dropouts, in which the energetic particle intensity decreases to background levels over

a time scale of minutes, are one example of steep cross-field gradients, which seem to imply a low ratio ($\kappa_{\perp}/\kappa_{\parallel} \sim 10^{-4}$), while large-scale modeling requires a high ratio ($\kappa_{\perp}/\kappa_{\parallel} \sim 10^{-2}$). We resolve this discrepancy by considering a field line meandering model together with high time cadence observations of the edges of dropouts. Furthermore, we more accurately determine the low-ratio value and find its energy dependence, and we show that this energy dependence is consistent with the results of quasilinear theory.

The Effect of Interplanetary Turbulence on Solar Energetic Particles

J. Giacalone*

Presenting and Corresponding Author: giacalon@lpl.arizona.edu

Energetic solar particles originate from near the Sun and are presumably accelerated by shock waves associated with solar eruptions such as flares or coronal mass ejections. Since these particles are observed far from the acceleration site, we must use remote observations to infer the processes responsible for their acceleration and propagation in space. A key finding is that the distribution of solar-energetic particles as a function of energy is usually a power law with a spectral exponent that does not vary greatly from one event to the next. The theory of diffusive shock acceleration robustly explains

this. However, a closer comparison of the predictions of the standard version of this theory with individual events rarely gives a one to one agreement. In this talk, I will address this by examining the role of interplanetary turbulence. I will show that single spacecraft time-series analysis of these events is not expected to show a nice agreement between theory and observations because of the stochastic nature of turbulence. When using two or more spacecraft that observe the same particle event, the agreement between theory and observation is much better.

Solar Cycle Dependence of Umbral Brightness and Magneto-Induced Line Broadening

T. Schad*

Presenting and Corresponding Author: tschad@lpl.arizona.edu

Studies of the disputed solar cycle dependence of peak umbral magnetic field strength have focused upon measurements of continuum intensity and line-of-sight (LOS) magnetic flux. Here we extend the discussion into a measurement of effective line width using eleven years of spectromagnetograms from the Kitt Peak Vacuum Telescope (KPVT) after revisiting core contrast measurements in order to more closely analyze dependence on umbral size. The KPVT observed the 868.8 nm Fe I absorption line in opposing states of circular polarization between 1992 and 2003, deriving full-disk images of LOS velocity, LOS magnetic flux, continuum intensity, equivalent line width, and central line depth. Spot selection is accomplished through an edge detection and thresholding algorithm. The resultant measurements are compared to previous measurements to verify accuracy. We determine an effective spectral line width through a relation of the measured equivalent line widths and central line depths. Developing

a basic model of the Stokes line profiles using the Seares formalism, we illustrate that a change in the effective line width within the umbra as determined using the KPVT data is consistent with the change in the effective width of the energy levels involved in Zeeman splitting. We discuss the effect of solar angle, stray light, as well as the unknown azimuthal angle of the magnetic field. Within individual sunspots observed near disk center, the determined effective line width decreases with distance from the central core consistent with the studied magnetic field gradient. Measurements of different sunspots show a clear dependence on umbral size consistent with previous studies of the umbral magnetic field. Using this effective line width as a diagnostic for magnetic field, we examine the possible dependence of maximum magnetic field strength on the phase of the solar cycle by way of a comprehensive statistical analysis of the largest number and temporal range of umbral measurements used to date.

Propagation of Impulsive Solar Energetic Particles in Large-Scale Turbulence

F. Guo* and J. Giacalone

Presenting and Corresponding Author: guofan@lpl.arizona.edu

Energetic Ions and Atoms from the Solar Wind Termination Shock

J. Kota*

Presenting and Corresponding Author: kota@lpl.arizona.edu

In December 2004, Voyager-1 reached a new frontier, the termination shock (TS), where the supersonic solar wind undergoes a shock transition. Beyond the shock, the interstellar wind deflects the subsonic solar wind and forces it to form an extended heliotail. Reaching the TS has long been awaited since the TS is a prime example of an astrophysical shock. Shocks are of great interest, they are believed to be responsible for accelerating charged particles to high energies, shock acceleration occurs near the Sun, at supernovae, and other places. The TS is where the so called anomalous cosmic rays (ACRs) are accelerated. The much anticipated shock-crossing brought surprises: contrary to expectations, the intensity of ACRs, did not unfold at the shock but continued to increase beyond the shock, which led some researchers

to questioning the basic paradigm of shock acceleration. In the talk I talk about possible interpretations, which do not require a new paradigm. We show that Voyager observations can be naturally interpreted in terms of shock acceleration.

Charge exchange between fast ions and slow neutral atoms can produce energetic neutral atoms (ENAs) which then move along ballistic trajectories free of the electromagnetic forces. ENAs can give a global map of the outer boundary regions of the heliosphere which is formed by the interaction between the solar wind and the interstellar medium. The Interstellar Boundary Explorer (IBEX) will be launched this summer to obtain such a global map of ENAs. I shall briefly discuss what IBEX can tell us on the structure of the heliosphere and on the physics of shock acceleration.

Terrestrial Planets and Titan

May 20
1:15PM – 2:30PM

Chair: C. Dundas

<i>Conference Schedule</i>	II
<i>Conference Welcome</i>	VI
<i>Science Abstracts, May 19</i>	
<i>Planetary Surfaces</i>	1
<i>Observation</i>	4
<i>Mars</i>	6
<i>Meteorites</i>	10
<i>User Demonstrations</i>	14
<i>Origins and Formation</i>	17
<i>Technical Abstracts, May 19</i>	
<i>Systems and Languages</i>	21
<i>Web Applications and Mission Planning Software</i>	23
<i>Data Archive</i>	26
<i>Data Analysis and Concurrency</i>	29
<i>Science Abstracts, May 20</i>	
<i>Dynamics</i>	32
<i>Atmospheres</i>	36
<i>Space Physics</i>	38
Terrestrial Planets and Titan	42
<i>Craters and Impacts</i>	46
<i>Satellites</i>	49
<i>Keynote</i>	52

Terrestrial Planet Formation: New Insights and Outstanding Questions

D. O'Brien*

Presenting and Corresponding Author: obrien@psi.edu

Invited Talk

Titan's Rain, Raindrops, and Dewdrops: Descent Imager / Spectral Radiometer Observations

E. Karkoschka* and M. Tomasko

Presenting and Corresponding Author: erich@pirl.lpl.arizona.edu

Titan was suspected to have an active methane cycle similar to the water cycle on Earth even before relevant observations were available to confirm the conjecture. In recent years, data have been streaming in. Discrete clouds were first inferred spectroscopically, but then also imaged by adaptive optics in the near infrared. Cassini provided high resolution images of clouds changing on times scales less than one hour. The descent of Huygens through Titan's atmosphere yielded one of the best local atmospheric data sets outside Earth. Measurements of temperature and the methane mixing ratio as functions of altitude lead to the possibility that it may have been drizzling during the descent.

The Descent Imager / Spectral Radiometer (DISR) on Huygens gave significant constraints about Titan's methane cycle. DISR images revealed no rain cloud, although we detected a dark layer at 21 km altitude. The layer was about 1 km thick and had an absorption optical depth of 0.001. It was only detectable near the horizontal direction from altitudes very close to 21 km, and only by special image processing. At least one similar, but even more subtle layer was detected at lower altitudes.

Our best explanation is a local enhancement of the aerosol size of the haze particles by a few percent. Considering that modeling of DISR data revealed a general increase of aerosol sizes from high altitudes to the surface, the 21-km layer may have had aerosols of similar size as at 20 km, but significantly larger than at 22 km.

In rain clouds, particle sizes grow by factors of about 1000 from micrometer sizes to millimeter sizes. Since DISR recorded accurately size variations by a few percent and did not record any larger variations, we can exclude the presence of drizzle or rain clouds near the trajectory of Huygens.

We simulated the visibility of rainbows for raindrops consisting of a mixture of methane and

ethane. Based on our unsuccessful search for a rainbow in DISR images, we put an upper limit for the optical depth of rain at 0.0002/km, which is much less than for a typical drizzle on Earth. This gives an upper limit for the drizzle rate during the Huygens descent of 0.0001 mm/h, which is 1 mm/year, much less than previous estimates of 10-100 mm/year.

We detected a few bright features on images taken after landing, which were only present in one image, but not in the other 82 images taken before or afterwards. An interpretation of these features as splashes of raindrops hitting Titan's surface had serious inconsistencies. Simulations with our data compression scheme argue that all but one of these features are probably cosmic ray hits.

One feature was very large and its structure was completely different from those caused by cosmic ray hits. We did theoretical calculations for the optics of the imager for various distances, where the camera is far out of focus. This was not tested in the laboratory since we expected the camera to work for distances of kilometers, not centimeters. For a distance of about 10 cm, the theoretical image looks much like the observed feature. We finally found a falling drop! It was illuminated by the DISR lamp. It seems we caught the two main reflections for a drop size of about 2 mm. The vertical smear during the exposure time is consistent with a falling speed of 0.5 m/s. It could not have been a raindrop since its trajectory would have needed to go through Huygens.

The drop was falling right below a baffle of the DISR camera, suggesting that we caught a dewdrop. Huygens warmed Titan's surface; warm, moist methane air originating from the surface was moving up along Huygens until it encountered the cold baffle of DISR, where it condensed. Many dewdrops fell down from the baffle, and one of them got caught during flight.

This work was supported by JPL Contract # 1279652.

Cassini Imaging of Titan and the Saturnian System

J. Perry*

Presenting and Corresponding Author: perry@pirl.lpl.arizona.edu

Hydrolysis of Laboratory Made Tholins in Ammonia-Water Solutions

C. Neish*, Á. Somogyi, J. Lunine, M. Smith

Presenting and Corresponding Author: cdneish@lpl.arizona.edu

Laboratory experiments that simulate the reactions occurring in Titan's thick nitrogen-methane atmosphere produce complex organic precipitates known as tholins. Tholins have the general formula $C_xH_yN_z$, and are spectrally similar to Titan's haze. When placed in liquid water, specific water soluble compounds in the tholins have been shown to produce oxygenated organic species with activation energies in the range of $\sim 60 \pm 10 \text{ kJ mol}^{-1}$ and half-lives between 0.3 and 17 days at 273 K (Neish et al. 2008). Oxygen incorporation into such materials – a necessary step towards the formation of biological molecules – is therefore fast compared to the freezing of impact melts and cryolavas on Titan.

The rates quoted above are for reactions occurring in pure liquid water. The composition of impact melts and lavas on Titan

are not likely to be pure water, but rather contain a few percent ammonia. Tobie et al. (2005) predict that Titan has a subsurface water layer with an ammonia concentration of 14 wt. % in the present era. The presence of ammonia would likely change the reaction rates and yields of the hydrolysis reactions of tholins. We have therefore extended our work to include the measurement of tholin hydrolysis rate coefficients in ammonia-water solutions. In this work, tholins were synthesized from a 0.98 N_2 /0.02 CH_4 atmosphere in a high voltage AC flow discharge reactor, and dissolved in a 14 wt. % ammonia-water solution. Rates were determined by monitoring intensity changes of select species over time using high resolution FT-ICR MS. Comparisons between rates of similar species observed at different pH will be presented.

Craters and Impacts

May 20
2:30PM – 3:00PM

Chair: C. Dundas

<i>Conference Schedule</i>	<i>II</i>
<i>Conference Welcome</i>	<i>VI</i>
<i>Science Abstracts, May 19</i>	
<i>Planetary Surfaces</i>	<i>1</i>
<i>Observation</i>	<i>4</i>
<i>Mars</i>	<i>6</i>
<i>Meteorites</i>	<i>10</i>
<i>User Demonstrations</i>	<i>14</i>
<i>Origins and Formation</i>	<i>17</i>
<i>Technical Abstracts, May 19</i>	
<i>Systems and Languages</i>	<i>21</i>
<i>Web Applications and Mission Planning Software</i>	<i>23</i>
<i>Data Archive</i>	<i>26</i>
<i>Data Analysis and Concurrency</i>	<i>29</i>
<i>Science Abstracts, May 20</i>	
<i>Dynamics</i>	<i>32</i>
<i>Atmospheres</i>	<i>36</i>
<i>Space Physics</i>	<i>38</i>
<i>Terrestrial Planets and Titan</i>	<i>42</i>
Craters and Impacts	46
<i>Satellites</i>	<i>49</i>
<i>Keynote</i>	<i>52</i>

Atmospheric Dispersion of Small Impacts on Mars

H.J. Melosh*, B.Ivanov, A. McEwen

Presenting and Corresponding Author: jmelosh@lpl.arizona.edu

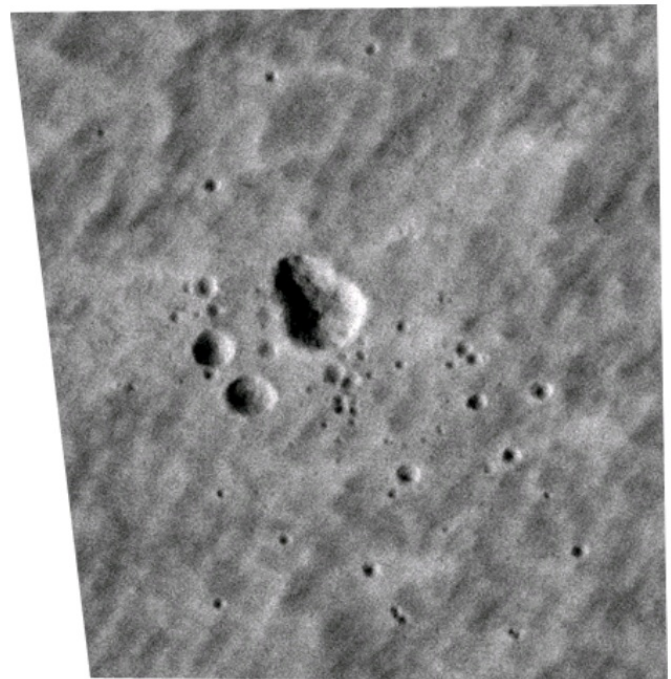
Introduction: In 2006 Malin et al [1], announced the discovery of 20 small dark areas on the surface of Mars that appeared to the MOC imaging system between 1999 and 2006. The size of the dark areas is on the order of a few km. The HiRISE imager aboard the Mars Reconnaissance Orbiter has now imaged all of these spots. At a resolution of approximately 30 cm/pixel, these dark spots are seen to surround small, fresh-appearing impact craters. With only a few exceptions, the craters form multiple clusters. The largest crater in each cluster ranges from 10 to 25 meters in diameter. If these are primary impactors, as appears most probable, these craters were caused by the impacts of primary objects in the size range of 1 to 3 meters diameter.

Crater Clusters: Only about one half of the craters imaged by HiRise are single. The other half of the small craters are clusters of several to several tens of visible craters that lie within about 100 m of each other. Two fields contain on the order of 10^3 to 10^4 craters near the limit of resolution that lie mostly within an elongated ellipse. Aside from the ellipse, there is no obvious sign of uprange-downrange polarity, unlike that seen in terrestrial and Venusian strewn fields, in which the largest crater usually falls downrange of the others due to atmospheric drag [2].

Implications for the Impactors: The theory of atmospheric breakup [3] suggests that a fast-moving meteorite that enters the atmosphere of a planet may be fractured by aerodynamic pressures proportional to $r_b v^2$, where r_b is the density of the atmosphere at the altitude of breakup and v is the entry velocity. The fragments disperse at a velocity proportional to the entry velocity times the ratio of r_b to the projectile density. As the fragments fall atmospheric drag on Earth further sorts the fragments by size, although this seems to have

not been important on Mars. The dispersion of the craters observed on Mars suggests breakup at an altitude of about 3 scale heights, implying that the incoming objects possessed strength on the order of 10^5 Pa and densities of 2000 to 3000 kg/m^3 , similar to that of most terrestrial meteors [4]. The widely dispersed fields suggest even lower densities: In a few cases models have a difficult time explaining the cluster's spread with even zero strength, unless the impacting object had a density on the order of 1000 kg/m^3 or less.

References: [1] Malin, M.C., Edgett, K.S., Posiolova, L.V., McColley, S.M. & Noe Dobrea, E.Z. (2006) *Science* **314**, 1573. [2] Passey, Q. & Melosh, H.J. (1980) *Icarus* **42**, 211. [3] Melosh, H.J. in *Multi-ring Basins* (eds. Schultz, P.H. & Merrill, R.B.) 29 (Pergamon, New York, 1981). [4] Svetsov, V.V., Nemtchinov, I.V. & Teterov, A.V. (1995) *Icarus* **116**, 131.



A small crater cluster found on HiRISE image PSP_005375

Bolide Impact as a Mechanism for Formation of Chaos Terrain on Europa

R. Cox*, L. Ong, M. Arakawa

Presenting and Corresponding Author: rcox@williams.edu

Chaos terrain on Europa may be caused by impact penetration of the ice crust. Ice thickness estimates and bolide dynamics at Europa indicate that some impacts not only crack the ice crust but fully breach it; and experiments show that projectiles impacting ice over water produce outcomes ranging from simple craters to open holes with floating ice rafts, depending on impact energy and ice thickness. First-order impacts—into thick ice or at low impact energy—produce craters. Second-order impacts punch through the ice, leaving clean-sided slush-filled holes that resemble raft-free (knobby) chaos. Third-order impacts—into thinnest ice or at highest energy—generate wide-field destruction, producing irregularly-shaped slush- and raft-filled impact zones similar to platy chaos. Other evidence for a relationship between chaos areas and impacts comes from the size-frequency distribution of chaos+craters on Europa, which matches the impact production functions of Ganymede and Callisto; and from the distribution of small craters around the large

chaos area Thera Macula, which decrease in areal density as a function of distance from Thera's centre.

On Europa, there are tiny craters 30 m in diameter, but no chaos areas less than ≈ 2 km across; and huge chaos areas more than 100 km across, but no craters even 50 km wide. This may reflect crustal thickness: small impactors never penetrate, whereas perhaps large ones (ÜberPenetrators, >2.5 km diameter at average impact velocity) always do. At intermediate sizes (2-40 km diameter) there are both craters and chaos, with craters more abundant at the smaller diameters and chaos dominating as size increases. This suggests that crust thickness varies, but that the larger the bolide, the greater the chance it will penetrate. If chaos areas represent impact sites, then Europa's surface is more impact-scarred than previously thought, and therefore older. The recalculated resurfacing age is 480 (-302/+960) Ma: greater than prior estimates, but still very young by solar system standards.

Satellites

May 20
3:15PM – 4:00PM

Chair: C. Neish

<i>Conference Schedule</i>	<i>II</i>
<i>Conference Welcome</i>	<i>VI</i>
<i>Science Abstracts, May 19</i>	
<i>Planetary Surfaces</i>	<i>1</i>
<i>Observation</i>	<i>4</i>
<i>Mars</i>	<i>6</i>
<i>Meteorites</i>	<i>10</i>
<i>User Demonstrations</i>	<i>14</i>
<i>Origins and Formation</i>	<i>17</i>
<i>Technical Abstracts, May 19</i>	
<i>Systems and Languages</i>	<i>21</i>
<i>Web Applications and Mission Planning Software</i>	<i>23</i>
<i>Data Archive</i>	<i>26</i>
<i>Data Analysis and Concurrency</i>	<i>29</i>
<i>Science Abstracts, May 20</i>	
<i>Dynamics</i>	<i>32</i>
<i>Atmospheres</i>	<i>36</i>
<i>Space Physics</i>	<i>38</i>
<i>Terrestrial Planets and Titan</i>	<i>42</i>
<i>Craters and Impacts</i>	<i>46</i>
Satellites	49
<i>Keynote</i>	<i>52</i>

Topography of Chaotic Terrain on Europa

R. Greenberg*, T. Hurford, K. Varland, M. Foley

Presenting and Corresponding Author: greenberg@lpl.arizona.edu

Many small patches of chaotic terrain on Europa appear to be bulged upward, which has contributed to qualitative impressions that chaos might represent “cryovolcanic” and/or convective upwelling. However, the oceanic melt-through model for chaos formation explains the bulged appearance differently as simply the topography expected after refreezing and buoyant equilibrium. Greenberg et al. suggested an observational test to discriminate between these models, based on whether or not the up-bulged chaos is higher than the typical tectonic terrain in the region (for up-welling) or only higher than its immediate moat-like surroundings (melt-through and refreezing). Several authors have taken up this challenge, presenting topographic maps to refute the melt-through model by showing high elevations for chaos. However, details on the methods (based on combinations of stereo images and photogrammetry) have been sketchy, and without quantitative discussion of uncertainties.

For example, near Tyre where high-resolution stereo is available, topographic maps and profiles have been used to refute the melt-through model. Yet the differences in elevations between various published results are over an order of magnitude greater than

the purported 10m precision. Moreover, high-elevation portions of profiles that were labeled as chaos are actually tectonic terrain. Stereo actually shows that major chaos areas are lower than the tectonic terrain in the area. Also, variations in elevation in the tectonic terrain itself are so great that any differences from chaotic terrain are in the noise. Moreover, we have performed analyses of uncertainties in both stereo and photogrammetry and find that both systematic and random errors are probably greater than any reported differences between elevations of chaotic and tectonic terrain. For example, stereo-based models may exaggerate the height of chaos by favoring rafts as tie features, and photogrammetry is sensitive to an uncertain photometric function and to sub-pixel slope variations, as we will demonstrate. We will also show how the stereo can be used to derive 3D shapes for the rafts in chaotic terrain.

To paraphrase Mark Twain, reports of the death of the melt-through model have been greatly exaggerated. Any results based on topography should not be accepted unless the methods involved have been subjected to rigorous and transparent quantitative evaluation.

Mission Concept: Io Volcano Observer (IVO)

A. McEwen* and the IVO Team

Presenting and Corresponding Author: mcewen@lpl.arizona.edu

This 6-month study is to evaluate the viability of IVO within the Discovery Program and with a government-furnished power system, specifically the Advance Sterling Radioisotope Generator (ASRG). The ASRG is 6 times more efficient in Watts per kg of Pu than conventional radioisotope generators, which is a major advantage given the scarcity of Pu. NASA wants to flight-test it first on a Discovery-class mission. We have just begun this study, but our preliminary plan is for a small Jupiter orbiter in a highly inclined orbit with periods ranging from 200 to 30 days and an Io flyby near each perijove. Functioning within the intense trapped radiation belts of Jupiter is a major challenge. The high inclination orbit reduces the total dose for each perijove pass, allows Io observations at closer range versus dose rate, and enables unique science observations. We are focused on a few key science objectives: (1) understand active volcanic processes (repeat observations with similar lighting and viewing conditions in color, stereo, and thermal), (2) determine

silicate lava compositions (measure peak temperatures and reflectance and/or emission spectroscopy), (3) constrain models for tidal heating (map global heat flow, measure satellite shape from limb fits, improved gravity data), and (4) better understand plume, atmospheric, Io plasma torus, and magnetospheric compositions and processes. We currently envision four baseline instruments: a Narrow-Angle Camera (NAC) with simultaneous color imaging, a Thermal Mapper (ThM) covering ~3, 8, and 15 microns and perhaps bandpasses for silicate compositions, a Neutral Mass Spectrometer (NMS), and a Radiation Detector (RaD). RaD will provide information useful to IVO operations and future Jupiter orbiters as well as magnetospheric science. Many other capabilities are desirable, such as a magnetometer, UV spectrometer, wide-angle camera, near-IR spectrometer, and ultra-stable oscillator. Unique polar monitoring of Jupiter would also be possible, limited by data rate.

Astrobotic and the Quest for the Google Lunar X-Prize

D. Lauretta*

Presenting and Corresponding Author: lauretta@lpl.arizona.edu

Keynote

May 20
4:00PM – 5:00PM

Chair: E. Cholle

<i>Conference Schedule</i>	II
<i>Conference Welcome</i>	VI
<i>Science Abstracts, May 19</i>	
<i>Planetary Surfaces</i>	1
<i>Observation</i>	4
<i>Mars</i>	6
<i>Meteorites</i>	10
<i>User Demonstrations</i>	14
<i>Origins and Formation</i>	17
<i>Technical Abstracts, May 19</i>	
<i>Systems and Languages</i>	21
<i>Web Applications and Mission Planning Software</i>	23
<i>Data Archive</i>	26
<i>Data Analysis and Concurrency</i>	29
<i>Science Abstracts, May 20</i>	
<i>Dynamics</i>	32
<i>Atmospheres</i>	36
<i>Space Physics</i>	38
<i>Terrestrial Planets and Titan</i>	42
<i>Craters and Impacts</i>	46
<i>Satellites</i>	49
Keynote	52

Icy Satellites: 400 Years of Discovery

M. Bland*

Presenting and Corresponding Author: mbland@lpl.arizona.edu

On January 7th of 1610, Galileo Galilei pointed his newly refined telescope at Jupiter and became the first person to observe its satellites. In a letter written that night Galileo declared, "this evening I have seen Jupiter accompanied by three fixed stars, totally invisible by their smallness. ... The planets are seen very rotund, like little full moons, and of a roundness bounded and without rays. But the fixed stars do not appear so..." [Drake, 1978]. By the time Galileo's discoveries were printed in *Sidereus Nuncius* on March 12 of that year, he had convinced himself that these "stars" were in fact orbiting Jupiter: "no one can doubt that they complete their revolutions about [Jupiter]. ... Our vision offers us four stars wandering around Jupiter like the Moon around the Earth ..." [Galilei, trans. 1989]. Galileo had initiated the study of satellites of the outer Solar System. Within half a century, satellites were discovered beyond Jupiter. In 1655 Christiaan Huygens discovered Saturn's largest satellite, Titan, and by the end of the century Giovanni Domenico Cassini had observed Saturn's next four largest satellites: Iapetus, Rhea, Dione, and Tethys. In the three centuries that followed Galileo's dramatic discovery, approximately 33 satellites with diameters greater than 100 km (including Galileo's) were discovered.

Direct exploration of the outer Solar

System and its satellites began with the launches of Pioneers 10 and 11 in 1972 and 1973, respectively. Though few measurements of icy satellites were made, the missions refined the masses of all four Galilean satellites and improved the diameter measurements of Callisto and Europa. It was not until Voyager I and II reached Jupiter in 1979, however, that our knowledge of icy satellites truly blossomed. The exploration of the outer Solar System continued with three additional missions: Galileo to Jupiter in 1989, Cassini-Huygens to Saturn in 1997, and New Horizons to Pluto in 2006. Through the data collected by these missions, a coherent, if complex, picture of icy satellites is now beginning to emerge.

Using the history of outer Solar System exploration as a framework, I will outline our current conception of icy satellites, emphasizing many of the first order questions that remain unaddressed.

References

- Drake, S. (1978). *Galileo at work, his scientific biography*. University of Chicago Press, Chicago.
- Galilei, G. (1989). *Sidereus Nuncius*. Translated by A. Van Helden. University of Chicago Press, Chicago.



© 2008 Lunar and Planetary Laboratory
Cover art by David Minton